Chapter 6

FAULT EVENTS DISTANCE ESTIMATION USING INTELLIGENT COMPUTING

6.1 Introduction

The neural networks are composed of large number of highly interconnected processing elements (neurons) working in unison to solve specific task. The performance of the network is mainly dependent on the applied connection weights. The designed network performs the specific task by regulating the values of the connecting weights in the network. In the recent few years, has been comprehensively applied in the different power system applications such as forecasting of loads, stability analysis and fault events detection [115-118]. In this chapter, an intelligent neural network based methodology has been presented for locating the fault events in the transmission system. The extracted feature vectors after DWT decomposition are fed to the designed distance estimator models for ascertaining the position of the faults in the network. The developed distance estimator model predicts the location of events in the transmission circuit as its output. Further, the strength and workability of the proposed fault distance estimating approach in the compensated transmission circuit is validated for different fault scenarios.

6.2 Fundamentals of Neural Network Models

Figure 6.1 shows the diagram of a single input neuron system without and with bias element. The input 'e' applied at the input layer is transmitted via a connection that multiplies its value by connecting weight 'w'. The utilized transfer function finally

produces the output of the system as 'a' which is simply function applied on 'we'. In the second system, as there is bias element present the final output of the system is transfer function applied on '$we+b$'.

$$a = f(we) \tag{6.1}$$

$$a' = f(we+b) \tag{6.2}$$

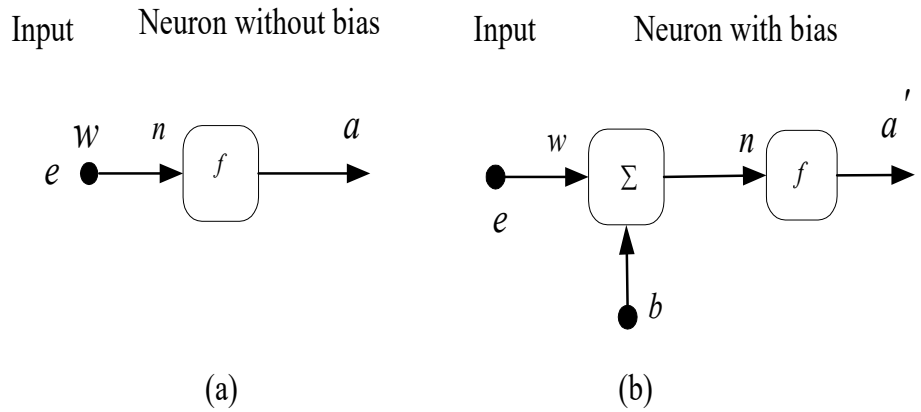

Figure 6.1 Single neuron structures (a) without bias (b) with bias

ANN is collections elementary neurons and it has three layers: input layer, hidden layer, and output layer. The feature vectors are applied to the input layer of the network. The second layer represents the key unit of the network. The neurons present in this layer processed and compute the applied input according to utilized weight vectors. It sends the final estimated values to the final output layer. The connecting weight vectors are regulated for mitigating the error between target and predicted value. On the basis of neurons interconnection in the model, the networks can be broadly categorized as feed-forward networks and feed-back networks. In the present work, following neural network models based distance estimator models have been designed for predicting the location of fault events in the transmission network-

i) Feed-forward neural network (FFNN)

ii) Linear neural network (LNN)

iii) Cascaded-forward neural network (CFNN)

iv) Generalized regression neural network (GRNN)

6.2.1 Feed-Forward Neural Network

In a feed-forward neural network each neuron in one layer has only directed connections to the neurons of the next layer (towards the output layer). The structure of feed-forward neural network is shown in Figure 6.2.

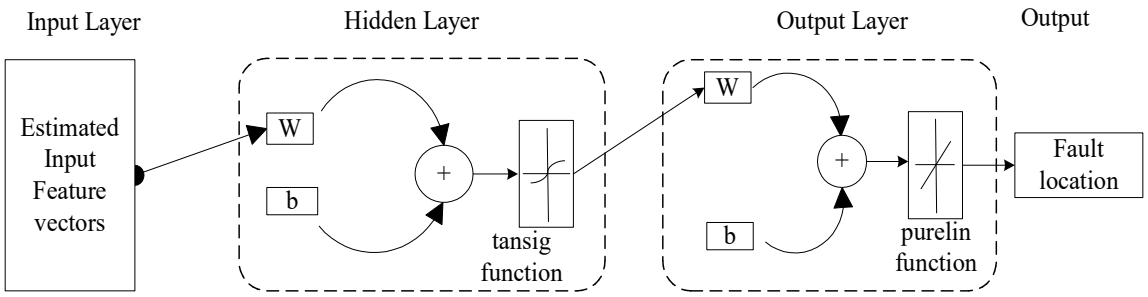

Figure 6.2 Architecture of feed-forward network

There are 10 neurons on hidden layer. Levenberg-Marquardt back propagation (trainlm) training function is used for the training of the neural network model. Although it requires more memory than other training algorithms but this algorithm will have the fastest convergence. Hyperbolic tangent sigmoid transfer function (tansig) is used for hidden layers and for the output layer linear transfer function (purelin) is used. The output layer consists of one output neuron representing fault location of the transmission line. Figure 6.3 (a) shows the (logsig) log-sigmoid transfer function; it produces output between 0 and 1as the neuron's net input goes negative to positive infinity. In multilayer networks the (tansig) tan-sigmoid transfer function shown in Figure 6.3 (b) is used.

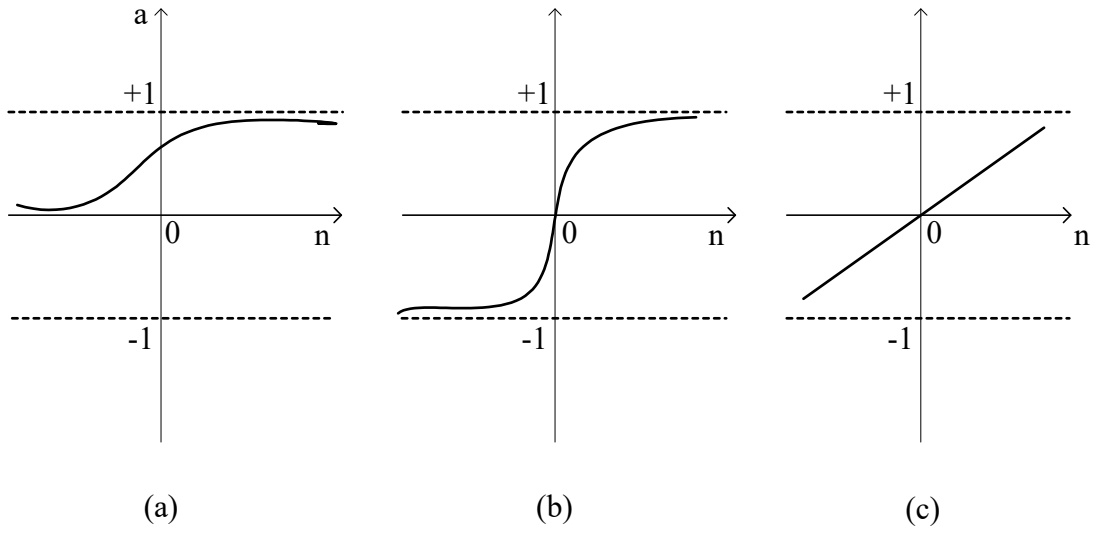

Figure 6.3 Activation transfer functions (a) log-sigmoid transfer function; (b) Tan-sigmoid transfer function; (c) purelin transfer function

The purelin transfer function shown in Figure 6.3 (c) is a linear function which estimates the neuron's output simply returning the value passed through it as given below-

$$a = purelin(we+b) = (we+b) \tag{6.3}$$

6.2.2 Linear Neural Network

LNN is similar to perceptron model; the only difference is it has linear transfer function instead of hard-limiting transfer function. This allows their outputs to take on any value, whereas the perceptron output is limited to either 0 or 1. The purelin transfer function is utilized in the output layer and it computes neurons output by returning the values passed to it. The extracted feature vectors are applied as input to the designed linear network and it predict the location of shunt fault event in the power transmission network as its output layer. The architecture of LNN is shown in Figure 6.4.

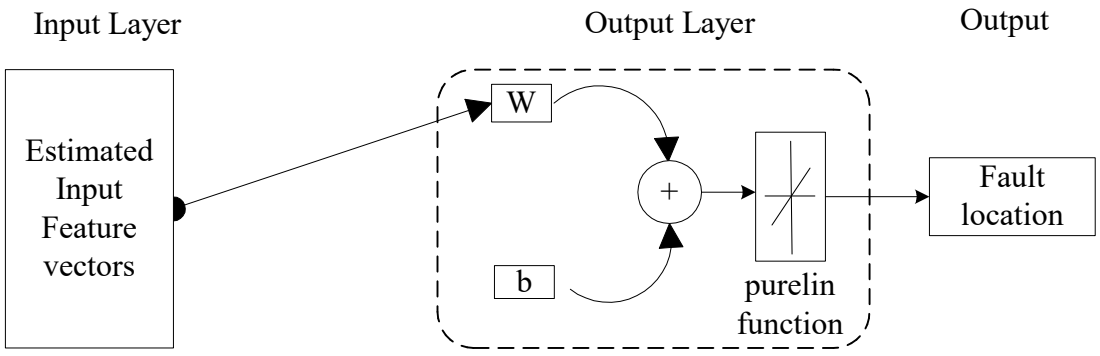

Figure 6.4 Architecture of linear neural network

6.2.3 Cascaded-Forward Neural Network

The CFNN model consists of three layers, i.e. input, hidden and output layer as same as feed-forward networks, but it has an additional weight connection from input to the consecutive layer and so on. The utilization of additional connection enhances the learning speed capability of the network. In the present work, Levenberg-Marquardt back propagation (trainlm) function has been used as the training function. The extracted feature vectors set are used as input to the designed CFNN model. Tansig transfer function has been used in the hidden layer for estimating hidden layer's output. In the output layer, purelin transfer function has been utilized. The output layer of the CFNN predicts the position of fault in the transmission network as its final output. Figure 6.5 shows the architecture of CFNN system.

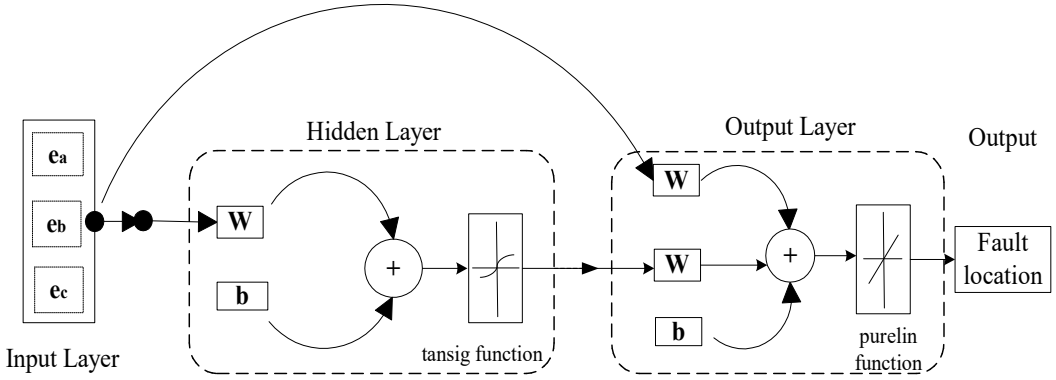

Figure 6.5 Architecture of CFNN

6.2.4 Generalized Regression Neural Network

GRNN is a type of radial basis network that is often used for function approximation. A feed-forward neural network with a single hidden layer that use a radial bias activation function for hidden neurons are called as radial basis function network. The architecture of GRNN is a combination of radial basis layer and a special linear layer. The first layer has as many radbas (Radial basis transfer function) neurons as there are input/target vector. It estimates the weighted inputs with || dist || and net input with netprod (net input function). The second layer has purelin neurons, it calculates weighted input with nprod (Normalized dot product), and net inputs with netsum (Sum net input function). The architecture for the GRNN is shown in Figure 6.6. The output layer, on the other hand consists of one output neuron representing fault location of the transmission line [119-120].

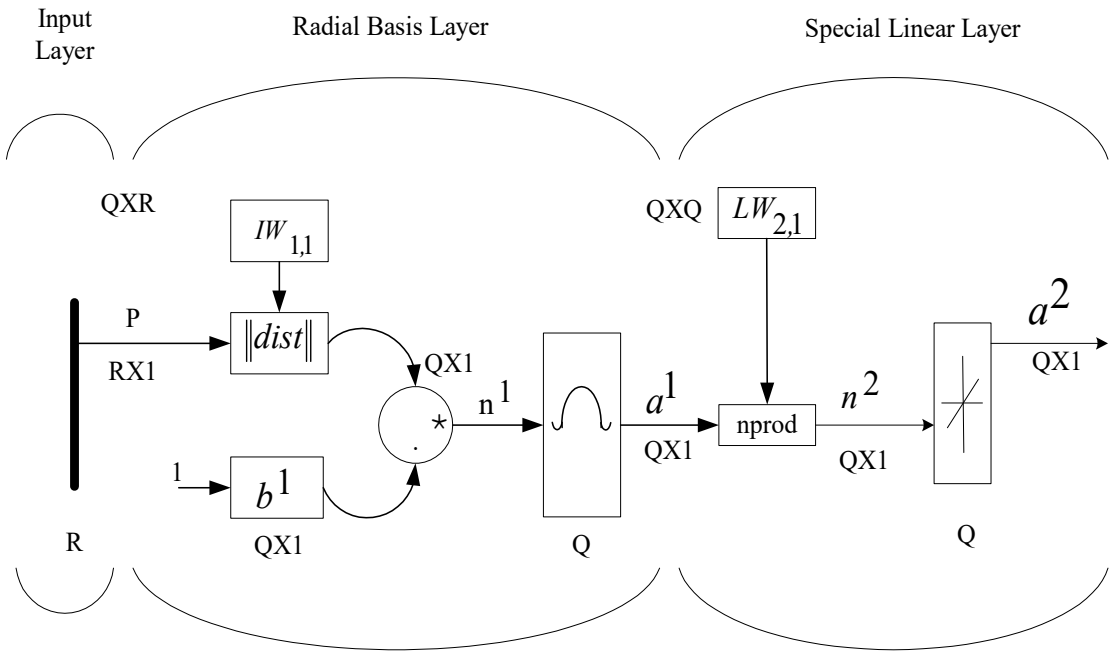

Figure 6.6 Architecture of GRNN

The radial basis function produces maximum of 1 when its input is 0. Hence a radial basis neuron acts as a detector which produces 1 whenever the input is identical to its weight vector. The bias *b* helps the sensitivity of the radbas neuron to be regulated. Figure 6.7 shows the radbas transfer function which gives output as-

$$radbas(n) = e^{-n^2} \tag{6.4}$$

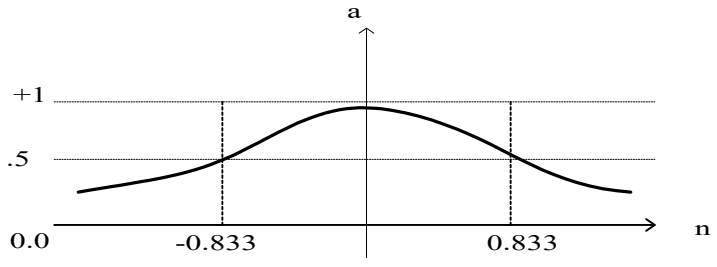

Figure 6.7 radbas transfer function

6.3 Proposed Intelligent Computing Based Fault Distance Estimation Methodology

The flow chart of the proposed integrated DWT and intelligent neural network model based scheme for ascertain the position of the fault events in the series compensated transmission system is shown in Figure 6.8. The extracted fault features after post fault current signal decomposition in terms of SD of detail coefficients (cD), norm entropy of the DWT coefficients, minimum and maximum value of the wavelet coefficients are utilized as the training and testing dataset in the designed neural network models. The detailed description of the applied mechanism and expressions for extracting the critical fault feature from the retrieved 3-phase post fault current signal is already discussed in second chapter. In the training phase, the computed feature vectors corresponding to various considered training fault scenarios in the simulated test systems are fed to the designed neural network based distance estimator models as the training dataset. Later on, during the testing the feature vectors associated with new unfamiliar fault events (considered testing cases) with varying circumstances are applied to the trained distance estimator models. The model predicts the estimated distance of the fault in the transmission system as its final output. In the present work, four distinct distance estimator models i.e. FFNN, LNN, CFNN, and GRNN are designed for predicting the location of fault events in the simulated series compensated power transmission system.

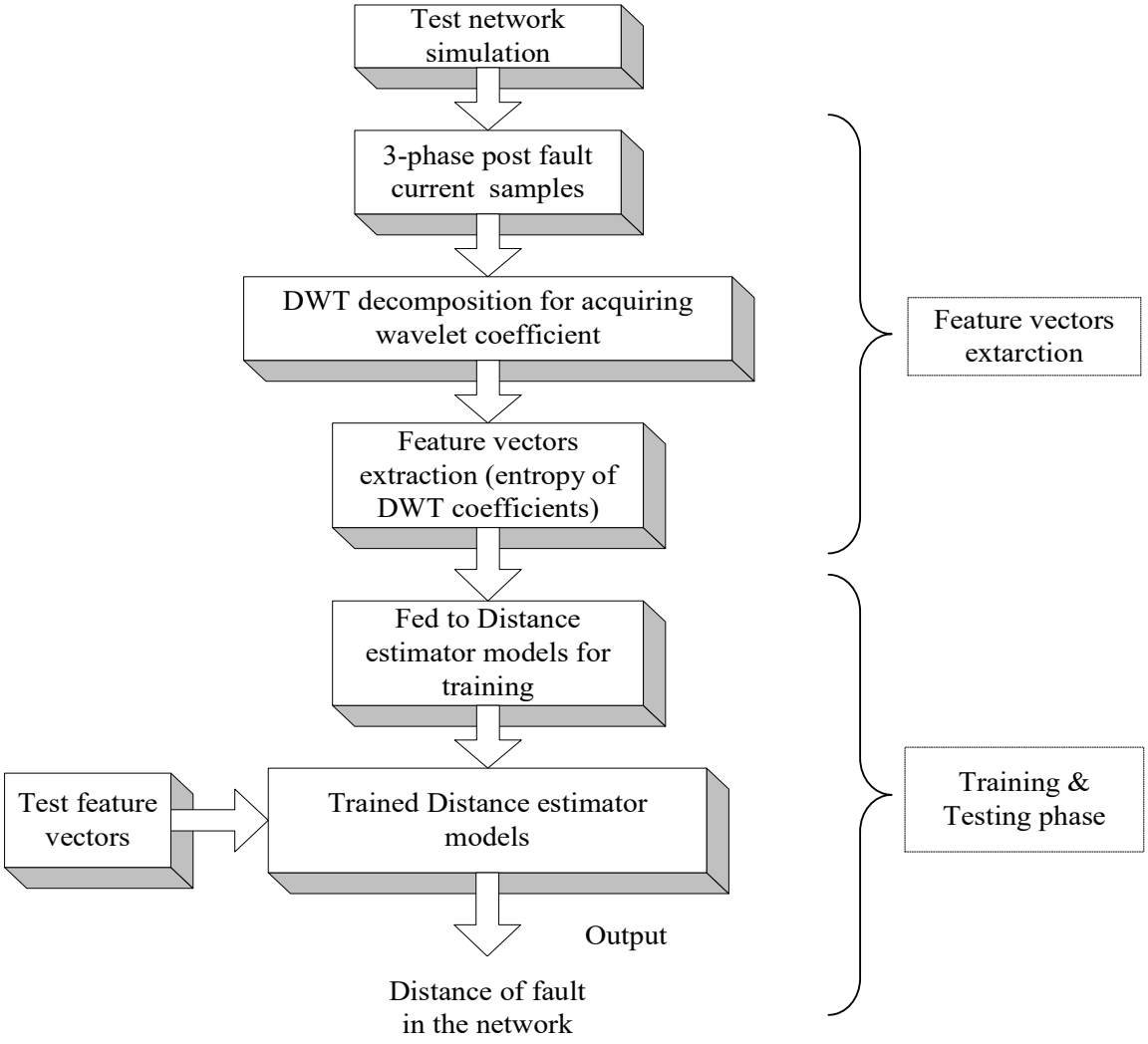

Figure 6.8 Flow-chart of the proposed fault location scheme

6.3.1 Training and Testing Mechanism

In the training phase, the computed fault features in terms of standard deviation of detailed coefficients (cD), norm entropy of the DWT coefficients, minimum and maximum value of the wavelet coefficients for various considered training fault scenarios in the simulated test system are applied to the designed distance estimator model. The considered training cases and conditions in the simulated test networks described in next section. The size of extracted input feature vector is 15 i.e. standard deviation of detail coefficients (cD) of 1st

and 5th decomposition level, norm entropy value of the wavelet coefficients and minimum and maximum value of the wavelet coefficients of each phase. The working details of the designed neural network based distance estimator models are already described in section 6.2. Levenberg-Marquardt back propagation (trainlm) function is utilized as the training function during the training. The tansig transfer function is utilized in the hidden layer for estimating hidden layer's output and purelin transfer function has been employed in the output layer. The output layer, of the distance estimator models has one neuron which represents the location of the fault events in the transmission lines. During the testing, the feature vectors corresponding to new unknown cases of fault events are applied to the trained classifier models. The trained distance estimator model predicts the particular location of the fault event in the transmission section on the basis of trained pattern set. The expression given in equation (6.2) has been utilized for assessing the fault distance estimation error in percentage.

$$\text{Distance Estimation}_{error}\left(\%\right)=\frac{\left(\text{Distance Estimator Model output}-\text{Actual location of fault}\right)}{\text{Length of line in km}}\times 100 \tag{6.2}$$

6.4 Case Study and Results

For assessing the feasibility of the proposed DWT and intelligent neural network based fault locating scheme in the series compensated transmission system, it has been extensively analysed for different fault scenarios in the simulated test networks. For training, the feature vectors corresponding to multiple fault events in a step of 5 km at different inception angles (0, 75, and 150 degree) and two level of line compensation are fed to the designed distance estimator model. In the testing phase, for tracing of the faults

position in the network, the features associated with different fault events at ten unknown places in the network, with varying conditions such as 4 different inception angles, two distinct line compensation levels have been applied to the trained distance estimator models. The neural network based distance estimator predicts the location of fault events in the network by comparing the input test feature instances with the trained pattern.

6.4.1 Test Case I: Two-Bus Series Compensated Transmission Test Network

For appraising the practicability of the proposed fault distance estimating scheme in series compensated transmission lines, it has been validated for various fault cases in the first test network. Figure 6.10 represents the 3-phase post fault current samples retrieved during different fault cases in the first simulated test network at 30 km from the sending side. During the testing, the feature vectors (i.e. SD of detail coefficients (cD) of 1st and 5^{th} decomposition level, norm entropy of DWT coefficients and minimum and maximum value of the wavelet coefficients of each phase) corresponding to all considered testing cases are fed to the trained distance estimator models for ascertaining the location of events in the transmission network. The distance estimator models predict the location of the test instance from the sending side as its output based on the trained pattern set. The fault distance estimation error has been computed using the expression given in equation 6.2.

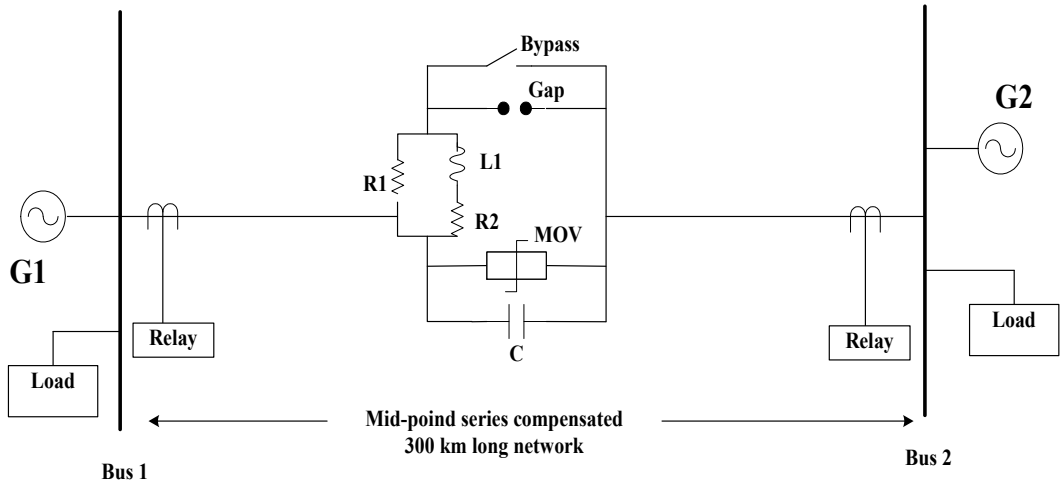

Figure 6.9 Two-bus mid-point compensated network (first test system)

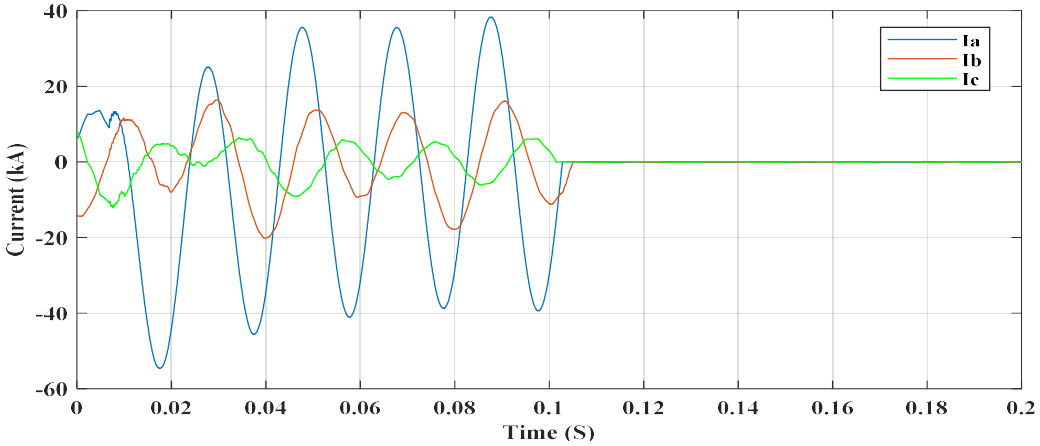

(a)

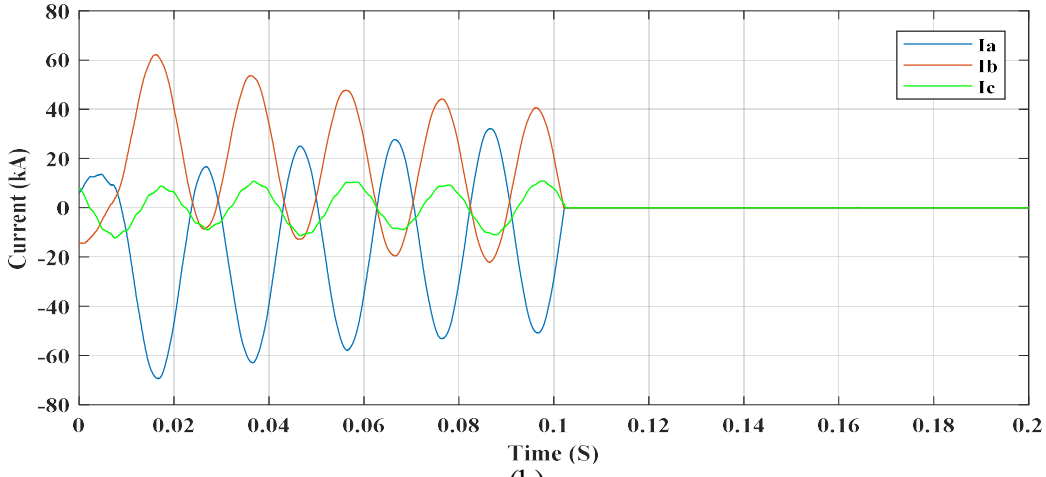

(b)

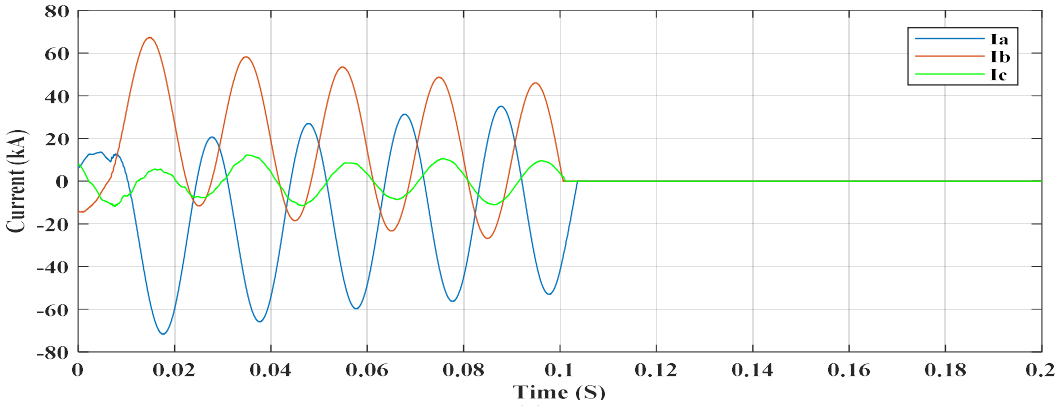

(c)

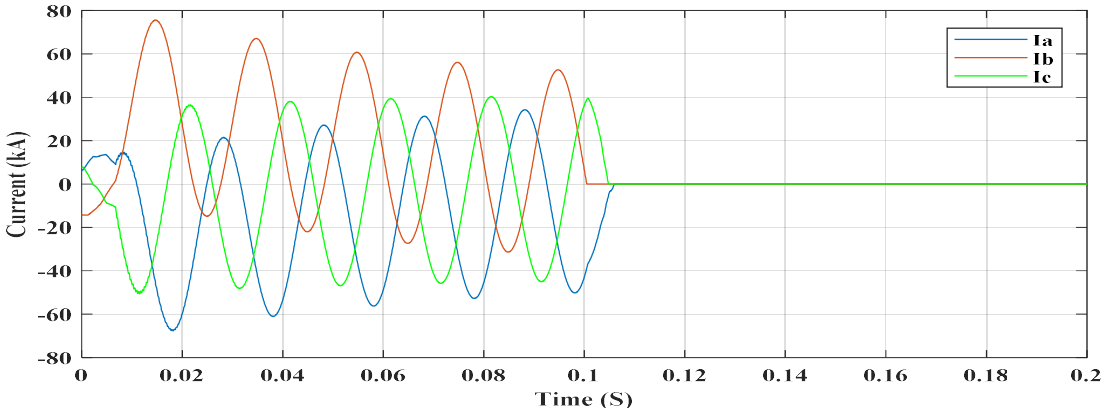

(d)

Figure 6.10 Three phase current signals during line different fault event at 30 km, 120 degree inception angle: (a) AG fault; (b) AB fault; (c) ABG fault; (d) ABC fault

Table 6.1-6.3 summarizes the fault distance estimation results and corresponding estimation error percentage provided by the FFNN, LNN and GRNN based distance estimator model during testing. It has been observed that the proposed scheme is well effective in ascertaining the location of the fault events in series compensated transmission system. Figure 6.11-6.13 represents the obtained error percentage during the tracing of different fault events in the simulated test network using FFNN, LNN, and GRNN respectively. The maximum distance assessment error is within 0.9 % for FFNN, 1.8 % for LNN, and 1.0 % for GRNN during testing in the transmission circuit.

Table 6.1 Fault events distance estimation using FFNN based distance estimator model

Type of fault	Actual location of fault	FFNN Model Output	Distance estimation Error (%)
Single line to ground fault	50	52.4752	0.8250
	90	91.9752	0.6584
	130	131.3797	0.4599
	190	190.6708	0.2236
	250	251.6981	0.5660
Double line fault	50	49.5927	0.1357
	90	91.8596	0.6198
	130	130.1578	0.0526
	190	190.4098	0.1366
	250	251.1506	0.3835
Double line to ground fault	50	52.5534	0.8511
	90	91.5159	0.5053
	130	131.9413	0.6471
	190	192.0037	0.6679
	250	251.7376	0.5792
Three-phase fault	50	51.2668	0.4222
	90	90.9403	0.3134
	130	128.7527	0.4157
	190	189.7336	0.0888
	250	249.8460	0.0513

Table 6.2 Fault events distance estimation using LNN based distance estimator model

Type of fault	Actual location of fault	LNN Model Output	Distance estimation Error (%)
Single line to ground fault	50	50.5040	0.168
	90	88.7912	0.4029
	130	129.5939	0.1353
	190	190.6367	0.2122
	250	250.8810	0.2936
Double line fault	50	48.7419	0.4193
	90	94.8953	1.6317
	130	133.8041	1.2680
	190	192.9698	0.9899
	250	250.0561	0.0187
Double line to ground fault	50	49.0408	0.3197
	90	88.4754	0.5082
	130	134.6198	1.5399
	190	195.3332	1.7777
	250	249.2739	0.2420
Three-phase fault	50	52.0097	0.6699
	90	88.3858	0.5380
	130	134.7701	1.5900
	190	186.4056	1.1981
	250	252.8415	0.9471

Table 6.3 Fault events distance estimation using GRNN based distance estimator model

Type of fault	Actual location of fault	GRNN Model Output	Distance estimation Error (%)
Single line to ground fault	50	51.8718	0.6239
	90	91.0893	0.3613
	130	130.0397	0.0132
	190	189.8104	0.0632
	250	249.6502	0.1166
Double line fault	50	50.3350	0.1116
	90	91.9999	0.6666
	130	128.7360	0.4213
	190	189.6397	0.1201
	250	250.0680	0.0226
Double line to ground fault	50	51.7718	0.5906
	90	92.0000	0.6666
	130	130.6284	0.2094
	190	191.9984	0.6661
	250	249.6107	0.1096
Three-phase fault	50	51.0673	0.3556
	90	91.2470	0.4156
	130	132.8541	0.9513
	190	189.7142	0.0952
	250	248.9360	0.3546

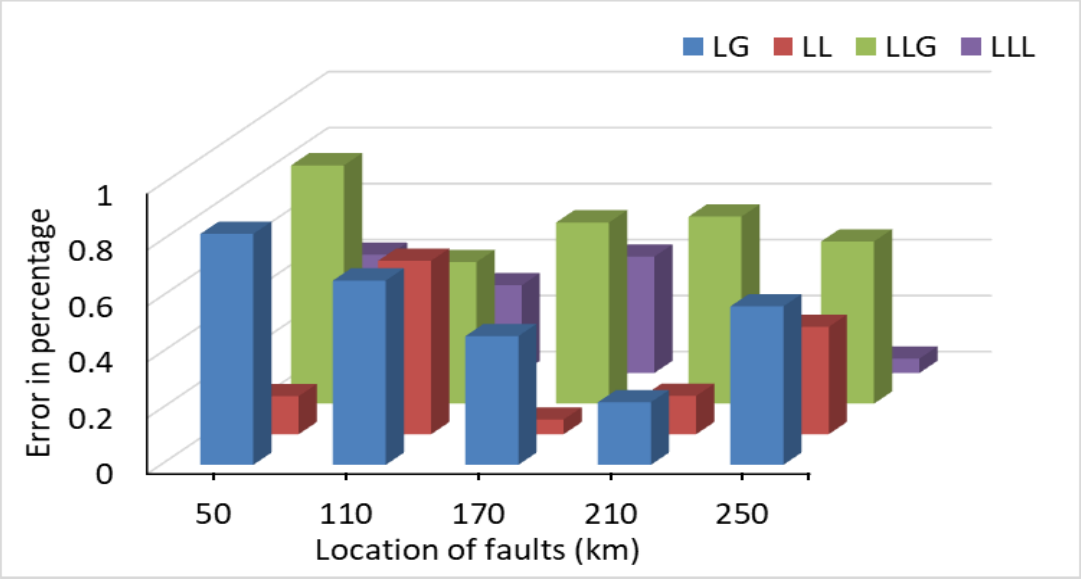

Figure 6.11 Distance estimation error percentage with respect to location of faults using FFNN

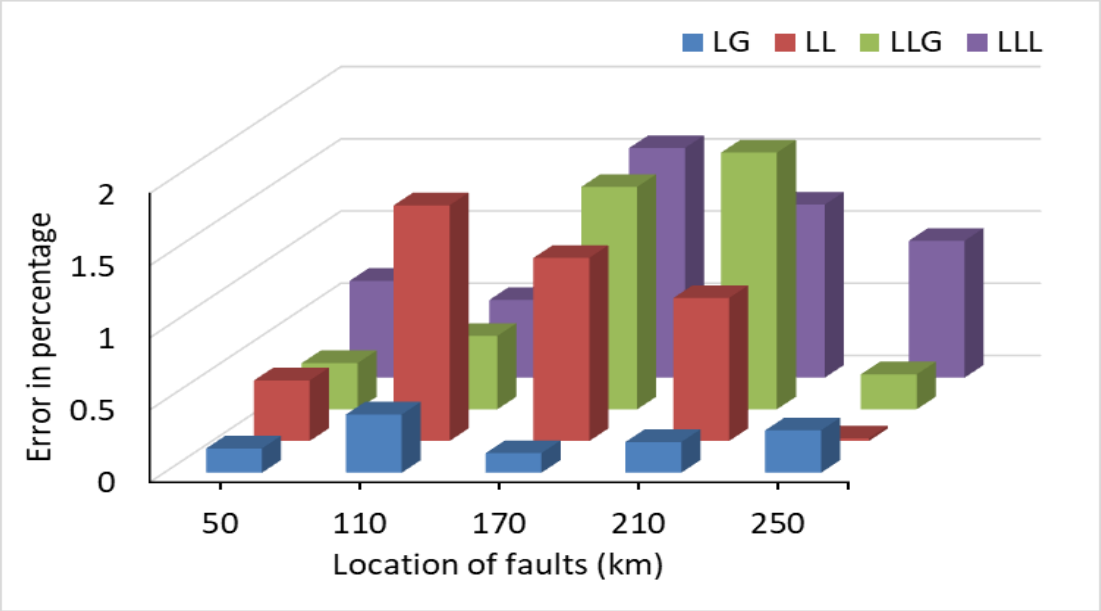

Figure 6.12 Distance estimation error percentage with respect to location of faults using LNN

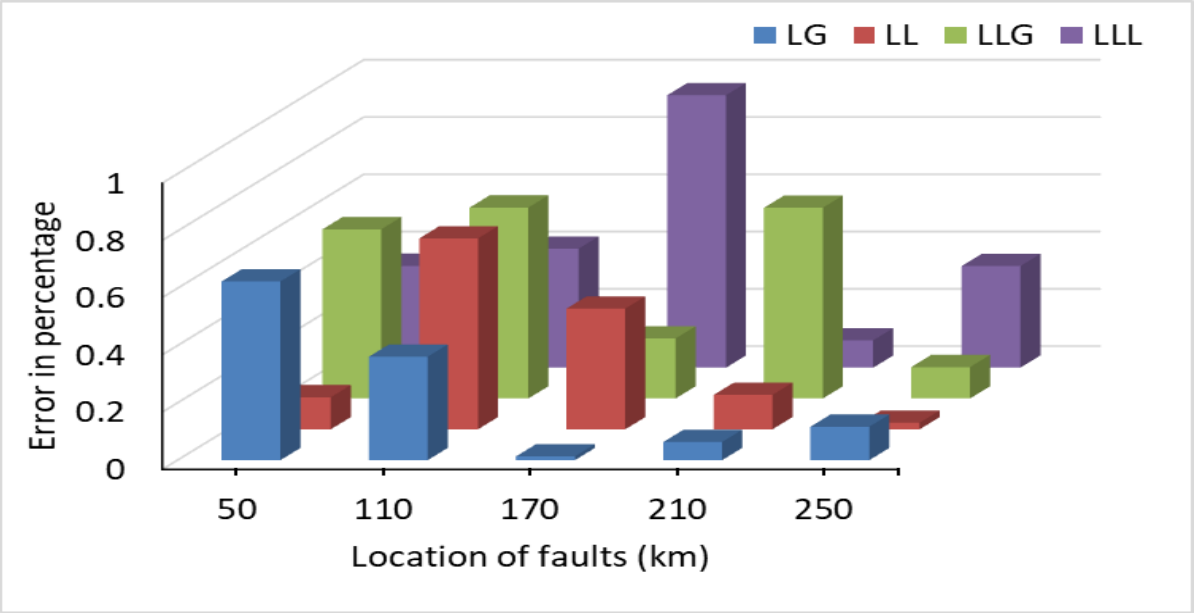

Figure 6.13 Distance estimation error percentage with respect to location of faults using GRNN

Table 6.4-6.5 summarizes the fault distance estimation results and corresponding estimation error percentage provided by the CFNN based distance estimator model during testing. It has been tested for various faults with varying inception angle and level of line compensation at ten different locations in the simulated test network. It shows that the proposed CFNN model based methodology is well effectual in ascertaining the location of the fault events in series compensated transmission system with high accuracy percentage. Figure 6.14 represents the obtained error percentage during the localization of different fault events in the 35 % compensated simulated test network on different inception angles. Similarly, Figure 6.15 represents the obtained error percentage during the tracing of different fault events in the 45 % compensated simulated test network on different inception angles. The maximum distance assessment error is within 1 % for all considered test events.

Table 6.4 Fault events distance estimation using CFNN model on different fault inception angles at 35 % of line compensation

Type of fault	Actual location of fault	CFNN Output 30-deg	Error (%)	CFNN output 60-deg	Error (%)	CFNN output 90-deg	Error (%)	CFNN output 120-deg	Error (%)
L-G	30	29.492	0.169	29.886	0.038	29.964	0.012	29.735	0.088
	50	50.307	0.102	49.840	0.053	50.027	0.009	49.868	0.044
	70	69.349	0.217	69.402	0.199	70.049	0.016	69.971	0.009
	90	89.722	0.092	90.212	0.070	90.154	0.051	89.304	0.232
	110	109.598	0.134	109.658	0.114	110.450	0.150	110.462	0.154
	130	129.512	0.162	129.853	0.049	130.578	0.192	130.270	0.090
	170	169.135	0.288	170.050	0.016	170.207	0.069	170.168	0.056
	190	190.151	0.050	189.692	0.102	189.958	0.014	189.623	0.125
	230	228.087	0.637	229.261	0.246	230.416	0.138	230.175	0.058
	250	250.867	0.289	249.421	0.193	249.586	0.138	250.971	0.323
L-L	30	30.097	0.032	29.570	0.143	29.263	0.345	30.428	0.142
	50	50.884	0.294	50.380	0.126	50.353	0.117	50.750	0.250
	70	70.251	0.083	69.783	0.072	67.827	0.724	69.472	0.176
	90	91.378	0.459	89.488	0.170	92.136	0.712	88.393	0.535
	110	109.212	0.262	110.858	0.286	109.748	0.084	110.364	0.121
	130	131.272	0.424	131.501	0.500	128.823	0.392	129.447	0.184
	170	169.550	0.150	170.859	0.286	169.186	0.271	171.392	0.464
	190	190.359	0.119	189.754	0.82	189.473	0.175	189.952	0.016
	230	229.226	0.258	231.622	0.540	227.594	0.802	228.493	0.502
	250	250.589	0.196	250.056	0.018	250.728	0.260	249.747	0.084
LL-G	30	29.211	0.263	30.603	0.201	29.405	0.198	29.717	0.094
	50	50.565	0.188	50.260	0.086	50.445	0.148	49.230	0.256
	70	71.954	0.651	70.002	0.0006	71.446	0.482	69.316	0.228
	90	89.523	0.159	90.688	0.229	92.908	0.964	90.676	0.225
	110	109.189	0.270	111.399	0.466	111.267	0.422	110.261	0.087
	130	132.249	0.749	131.355	0.451	131.294	0.431	130.875	0.291
	170	169.725	0.091	171.702	0.567	169.869	0.043	169.426	0.191
	190	189.628	0.124	190.343	0.114	191.075	0.358	190.140	0.046
	230	229.429	0.190	230.878	0.292	229.840	0.053	229.858	0.047
	250	249.429	0.190	250.306	0.102	250.233	0.077	249.546	0.151
LLL	30	30.518	0.172	30.350	0.116	30.225	0.075	30.3724	0.124
	50	50.885	0.295	49.263	0.245	48.942	0.352	49.584	0.138
	70	70.651	0.217	70.769	0.256	69.373	0.209	70.503	0.167
	90	92.846	0.948	89.031	0.323	89.310	0.230	90.910	0.303
	110	110.338	0.112	109.705	0.098	109.150	0.283	110.093	0.031
	130	131.021	0.340	127.306	0.898	130.066	0.022	128.649	0.450
	170	170.171	0.057	170.213	0.071	169.957	0.014	170.527	0.175
	190	191.242	0.414	190.705	0.235	191.336	0.445	190.343	0.114
	230	230.293	0.097	228.858	0.380	230.183	0.061	230.022	0.007
	250	250.305	0.101	249.581	0.139	251.485	0.495	250.255	0.085

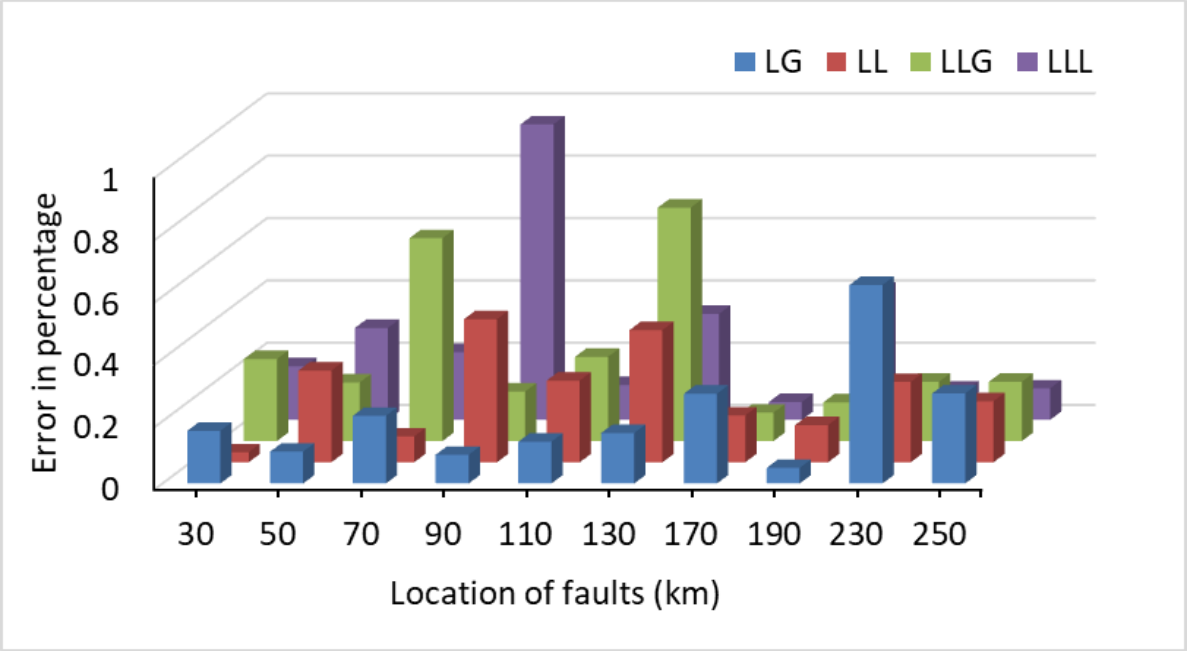
LG
LL
LLG
LLL
Error in percentage
1
0.8
0.6
0.4
0.2
0
30
50
70
90
110
130
170
190
230
250
Location of faults (km)

(a)

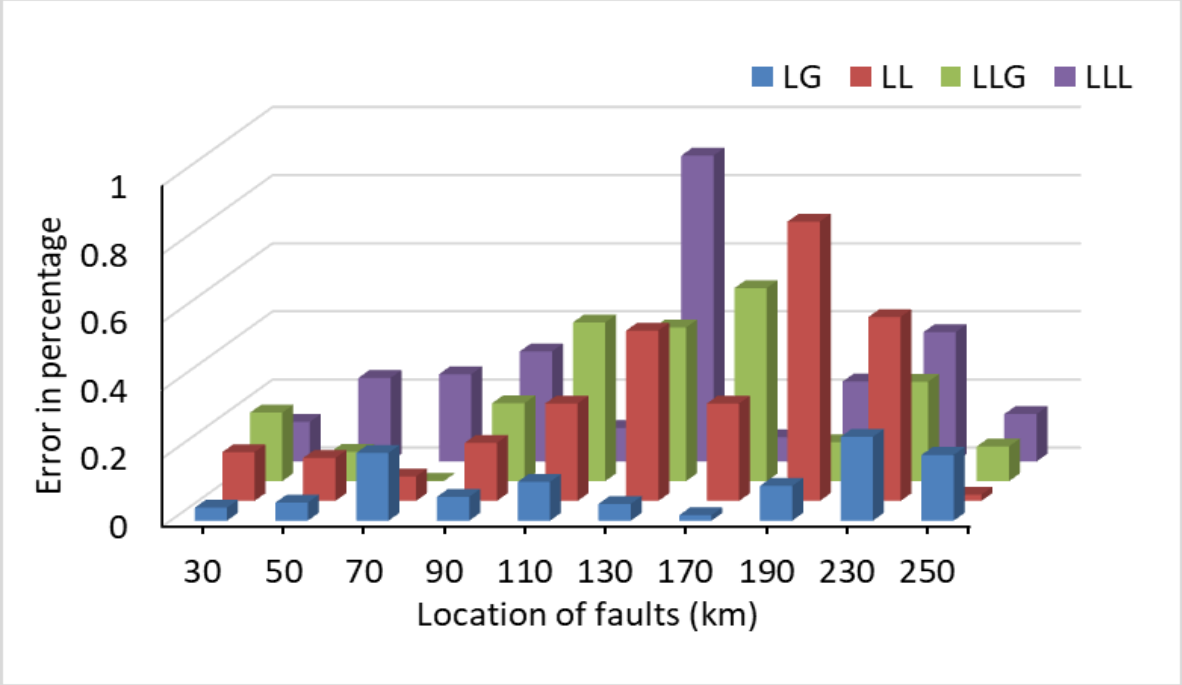
LG
LL
LLG
LLL
Error in percentage
1
0.8
0.6
0.4
0.2
0
30
50
70
90
110
130
170
190
230
250
Location of faults (km)

(b)

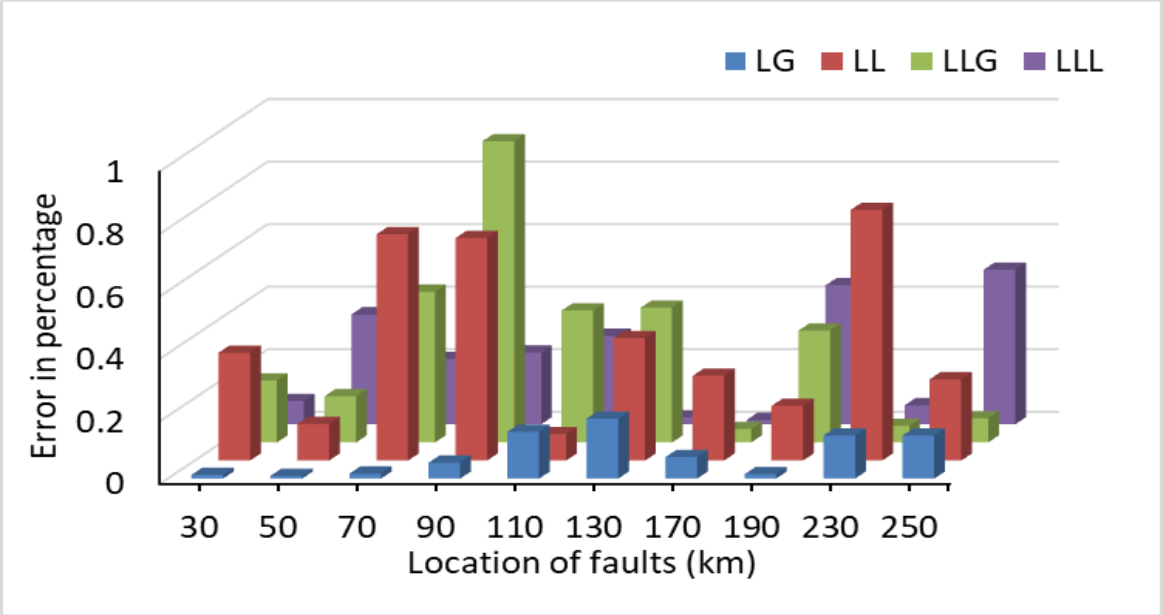

(c)

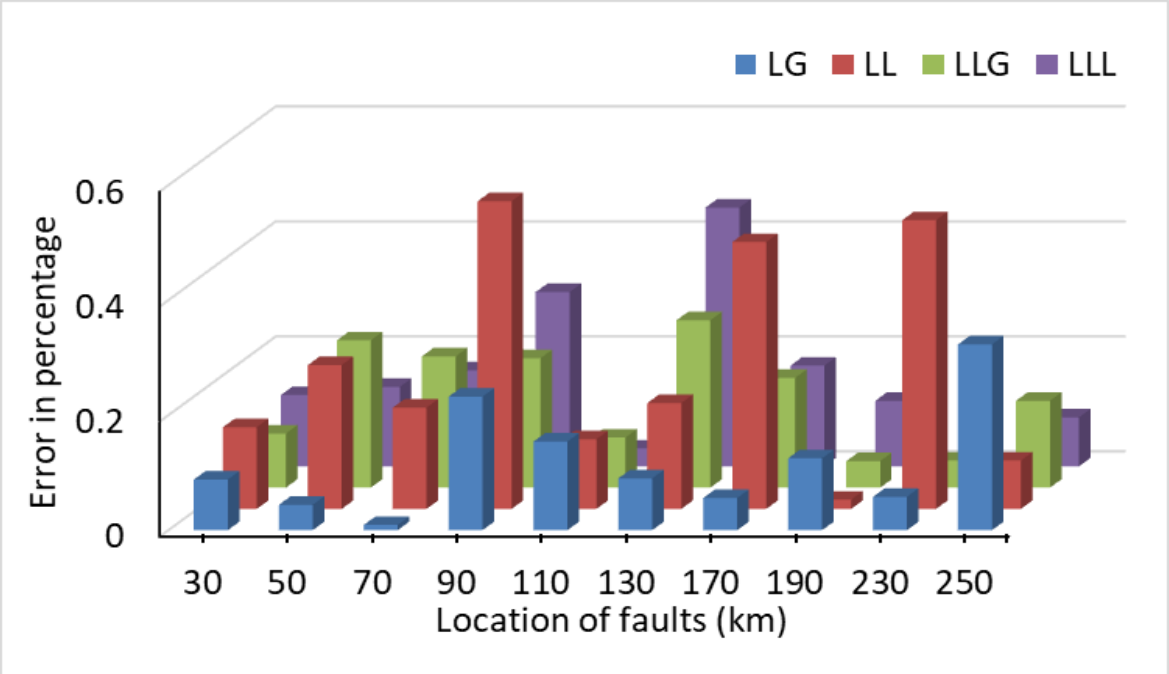

(d)

Figure 6.14 Distance estimation error percentage with respect to location of faults using CFNN at 35 % compensation of line on different inception angles: (a) 30 degree (b) 60 degree (c) 90 degree and (d) 120 degree

Table 6.5 Fault events distance estimation using CFNN model on different fault inception angles at 45 % of line compensation

Type of fault	Actual location of fault	CFNN Output 30-deg	Error (%)	CFNN output 60-deg	Error (%)	CFNN output 90-deg	Error (%)	CFNN output 120-deg	Error (%)
L-G	30	30.278	0.092	30.264	0.088	29.019	0.327	29.797	0.067
	50	49.727	0.091	50.613	0.204	49.209	0.263	50.664	0.221
	70	69.722	0.092	69.781	0.073	69.722	0.092	69.861	0.046
	90	89.278	0.240	89.281	0.239	89.248	0.250	89.321	0.226
	110	110.181	0.060	110.053	0.017	109.278	0.240	110.637	0.212
	130	130.193	0.064	129.258	0.247	130.319	0.106	130.186	0.062
	170	169.397	0.201	170.666	0.222	170.342	0.114	169.741	0.086
	190	189.504	0.165	190.453	0.151	189.590	0.136	189.295	0.235
	230	229.812	0.062	229.593	0.135	229.066	0.311	229.485	0.171
	250	249.130	0.29	249.714	0.095	250.023	0.007	251.210	0.403
L-L	30	29.608	0.130	30.420	0.14	30.232	0.077	30.203	0.067
	50	51.169	0.389	50.613	0.204	48.649	0.450	50.419	0.139
	70	71.910	0.636	70.265	0.088	72.639	0.879	69.214	0.262
	90	89.600	0.133	91.357	0.452	89.473	0.175	90.267	0.089
	110	109.349	0.217	110.317	0.105	110.908	0.302	109.296	0.234
	130	129.379	0.207	131.642	0.547	130.415	0.138	131.573	0.524
	170	169.536	0.154	169.040	0.32	170.803	0.267	169.584	0.138
	190	190.379	0.126	190.773	0.257	189.792	0.069	189.601	0.133
	230	231.670	0.556	230.188	0.062	232.299	0.766	231.573	0.524
	250	249.454	0.182	250.971	0.323	250.031	0.010	250.774	0.258
LL-G	30	30.345	0.115	29.442	0.186	29.575	0.141	30.153	0.051
	50	50.264	0.088	49.841	0.053	50.815	0.271	49.475	0.175
	70	71.028	0.342	72.572	0.857	72.958	0.986	72.602	0.867
	90	91.573	0.524	87.997	0.667	88.444	0.518	90.380	0.126
	110	109.255	0.248	110.156	0.052	110.423	0.141	109.669	0.110
	130	128.948	0.350	131.294	0.431	130.573	0.191	131.066	0.355
	170	169.574	0.142	170.065	0.021	172.306	0.768	168.934	0.355
	190	191.044	0.348	189.833	0.055	190.144	0.048	190.290	0.096
	230	229.228	0.257	231.803	0.601	230.226	0.088	230.910	0.303
	250	249.397	0.201	249.864	0.045	249.405	0.198	250.841	0.280
LLL	30	30.715	0.238	29.692	0.102	30.568	0.189	29.894	0.035
	50	50.671	0.223	49.210	0.263	48.976	0.341	49.911	0.029
	70	68.905	0.365	70.412	0.137	70.472	0.157	71.312	0.437
	90	89.249	0.250	88.280	0.573	90.678	0.226	87.703	0.765
	110	110.879	0.293	109.139	0.287	107.109	0.963	110.511	0.170
	130	132.348	0.782	129.912	0.029	130.396	0.132	129.132	0.289
	170	169.929	0.023	168.911	0.363	171.832	0.610	170.501	0.167
	190	188.491	0.503	190.281	0.093	192.089	0.696	189.236	0.254
	230	229.178	0.274	229.218	0.260	231.704	0.568	228.006	0.664
	250	248.732	0.422	249.513	0.162	250.919	0.306	247.762	0.746

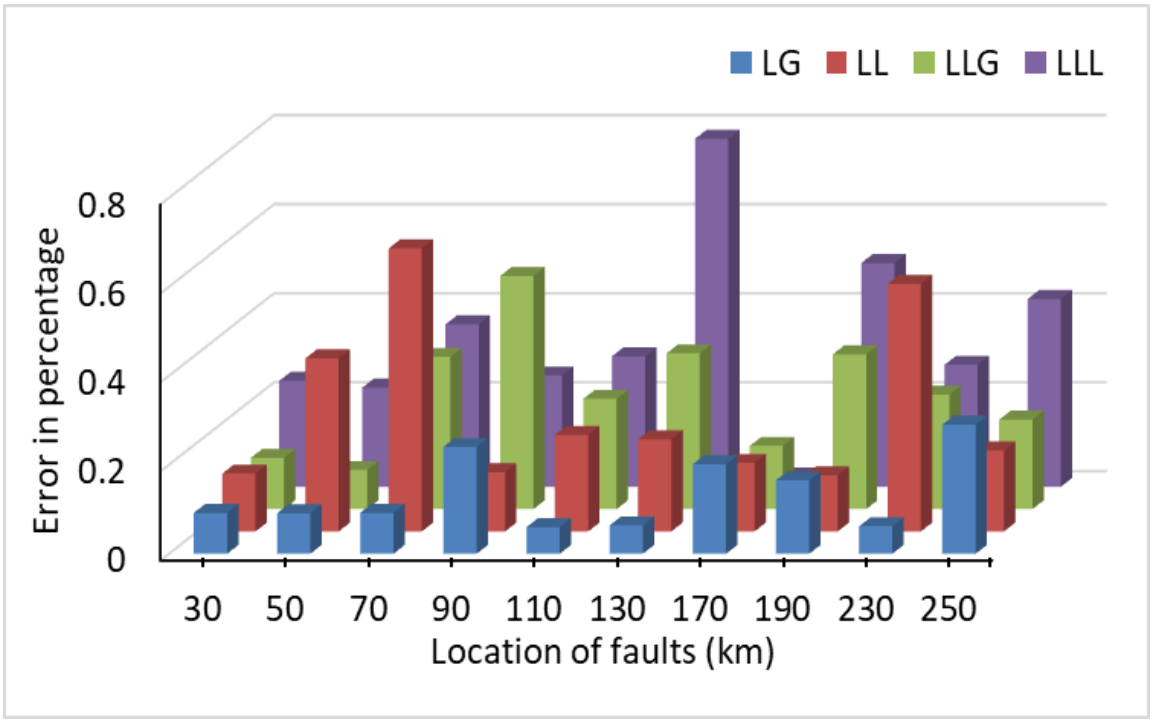
LG
LL
LLG
LLL
Error in percentage
0
0.2
0.4
0.6
0.8
30
50
70
90
110
130
170
190
230
250
Location of faults (km)

(a)

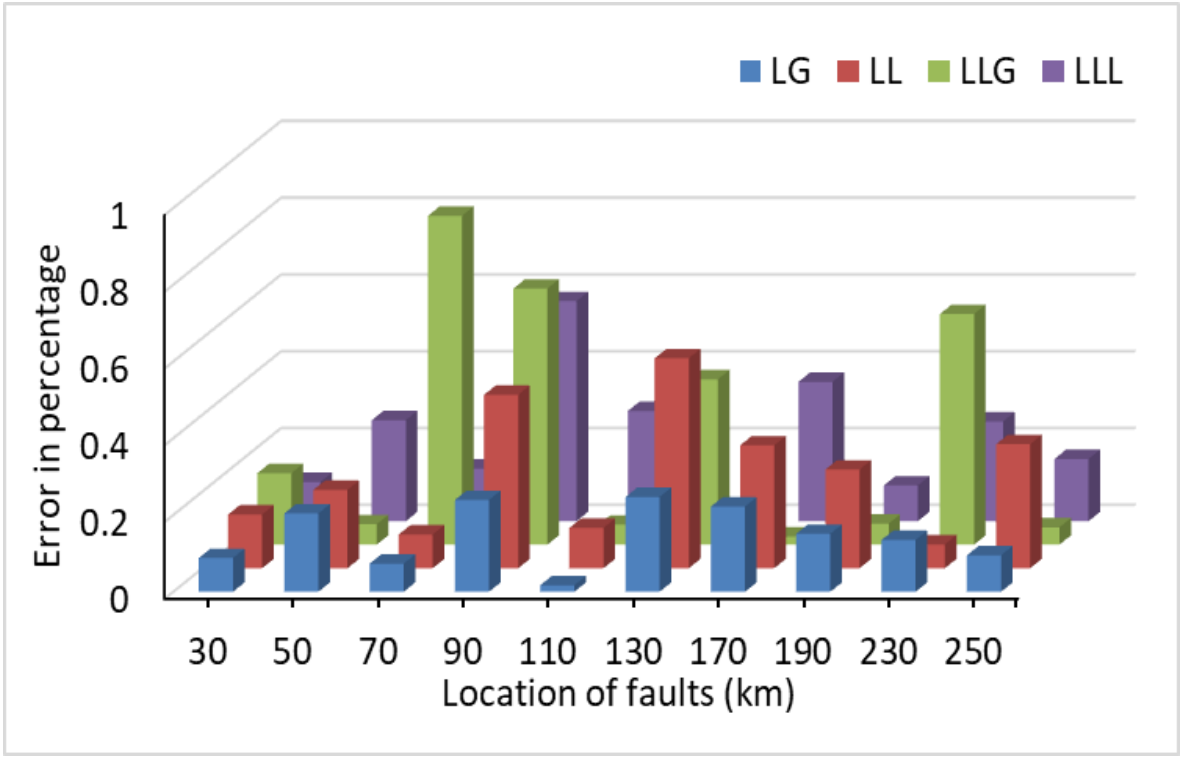
LG
LL
LLG
LLL
Error in percentage
0
0.2
0.4
0.6
0.8
1
30
50
70
90
110
130
170
190
230
250
Location of faults (km)

(b)

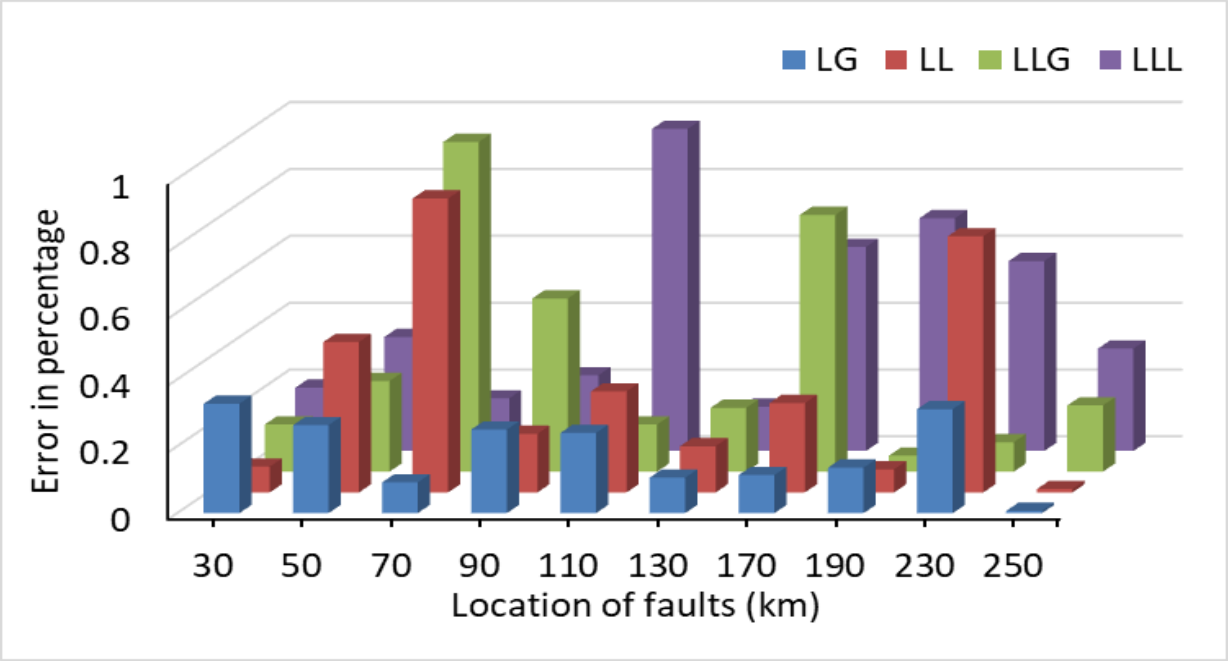

(c)

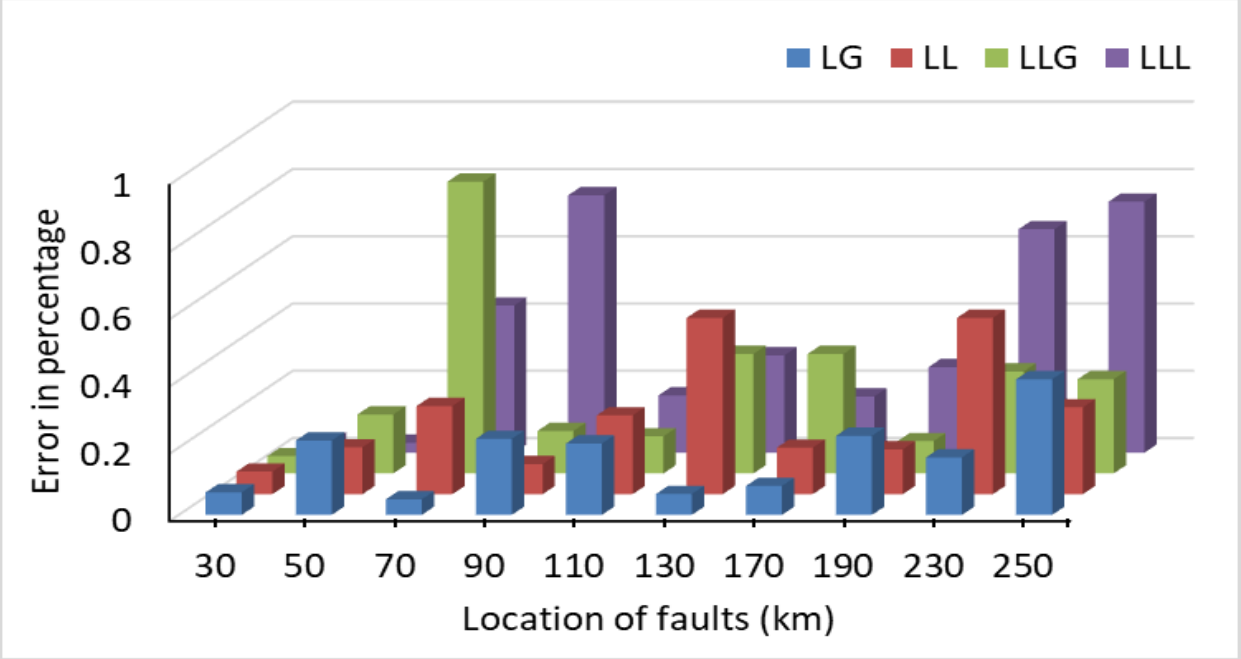

(d)

Figure 6.15 Distance estimation error percentage with respect to location of faults using CFNN at 45 % compensation of line on different inception angles: (a) 30 degree (b) 60 degree (c) 90 degree and (d) 120 degree

6.4.2 Test Case II: Modified IEEE 9-Bus Series Compensated Test Network

The ability of the proposed CFNN based fault distance estimating scheme has been also validated on second simulated test network (shown in Figure 6.16). It has been tested for distinct fault cases at five different locations in the transmission network. Figure 6.17 shows the 3-phase post fault current samples retrieved during different fault cases in the first simulated test network at 30 km from the sending side. During the testing, the features corresponding to all considered testing cases are fed to the trained distance estimator models. It predicts the location of the test instance in the network as its output based on the trained pattern set.

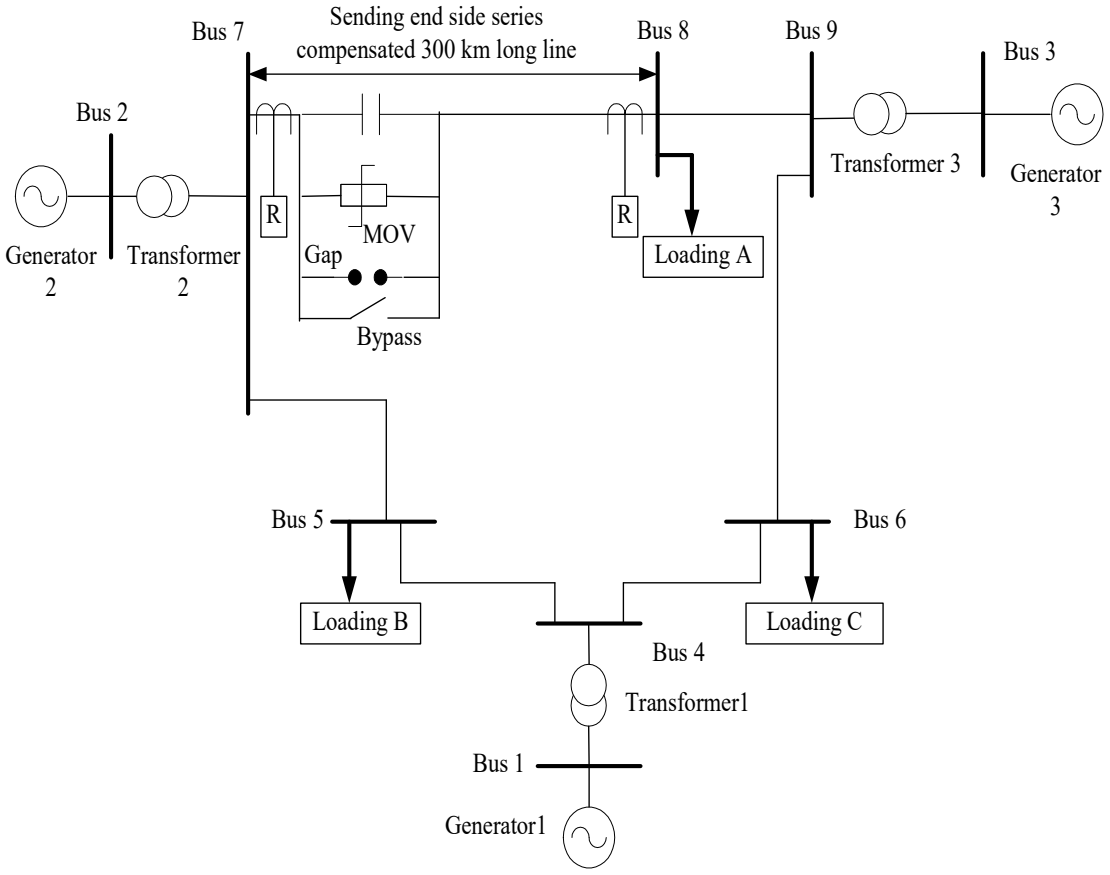

Figure 6.16 Simulated modified WSCC 9-Bus IEEE network (second test system)

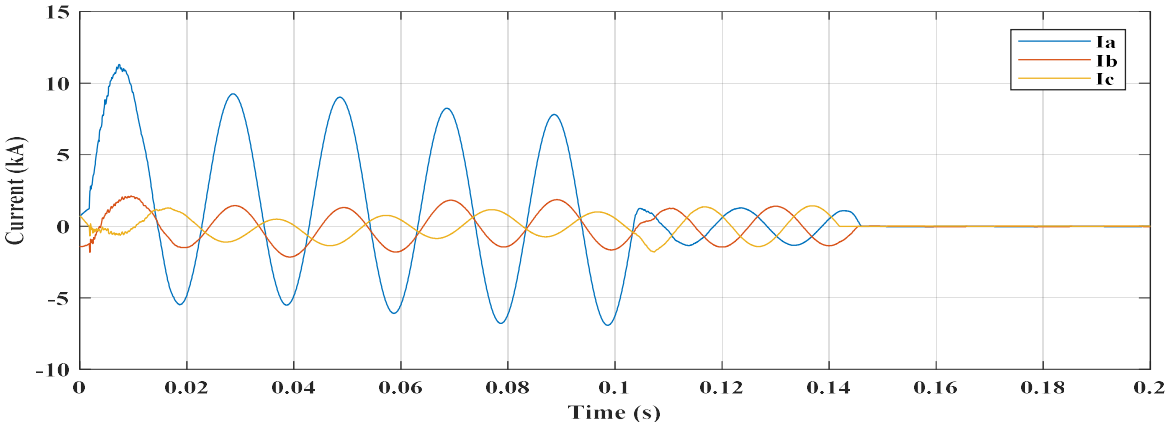

(a)

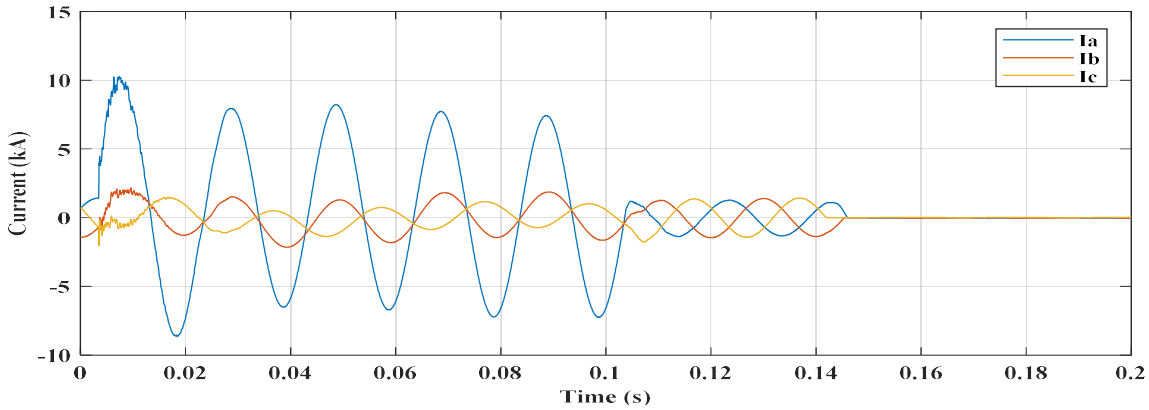

(b)

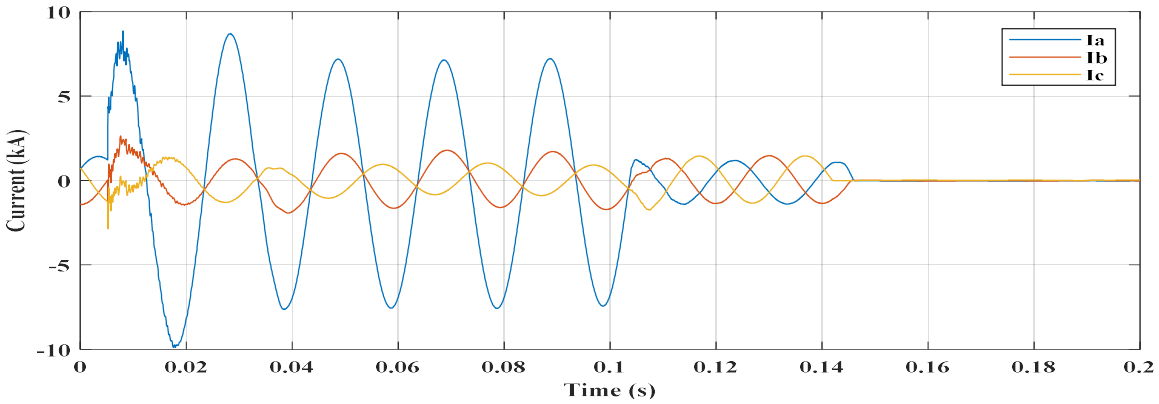

(c)

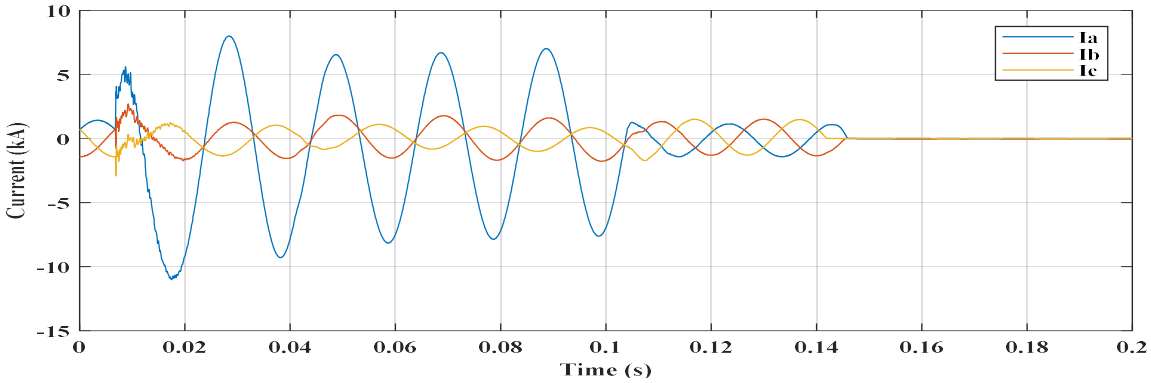

(d)

Figure 6.17 Three phase current signals during line to ground fault event at 50 km on different inception angles (a) 30 degree; (b) 60 degree; (c) 90 degree; (d) 120 degree

Table 6.6 summarizes the fault distance estimation results and corresponding estimation error percentage acquired by using the proposed CFNN based distance estimating scheme. The obtained results clearly vindicated that the proposed CFNN based scheme is well competent in ascertaining the position of fault events in series compensated transmission system. Figure 6.18 represents the obtained error percentage during the tracing of different fault events in the simulated test network. The maximum distance assessment error is within 0.5 % by the proposed CFNM model based distance estimator model.

Table 6.6 Fault events distance estimation using CFNN model on second test system

Type of fault	Actual location of fault	CFNN Model Output	Distance estimation Error (%)
Single line to ground fault	50	49.271	0.243
	110	109.643	0.119
	170	170. 325	0.108
	210	209.414	0.195
	250	249.350	0.216
Double line fault	50	50.635	0.211
	110	111.320	0.440
	170	169.436	0.188
	210	209.539	0.153
	250	250.424	0.141
Double line to ground fault	50	49.672	0.109
	110	110.826	0.275
	170	170.628	0.209
	210	211.394	0.464
	250	249.310	0.230
Three-phase fault	50	51.067	0.355
	110	109.640	0.120
	170	171.254	0.418

	210	209.214	0.262
	250	248.736	0.421

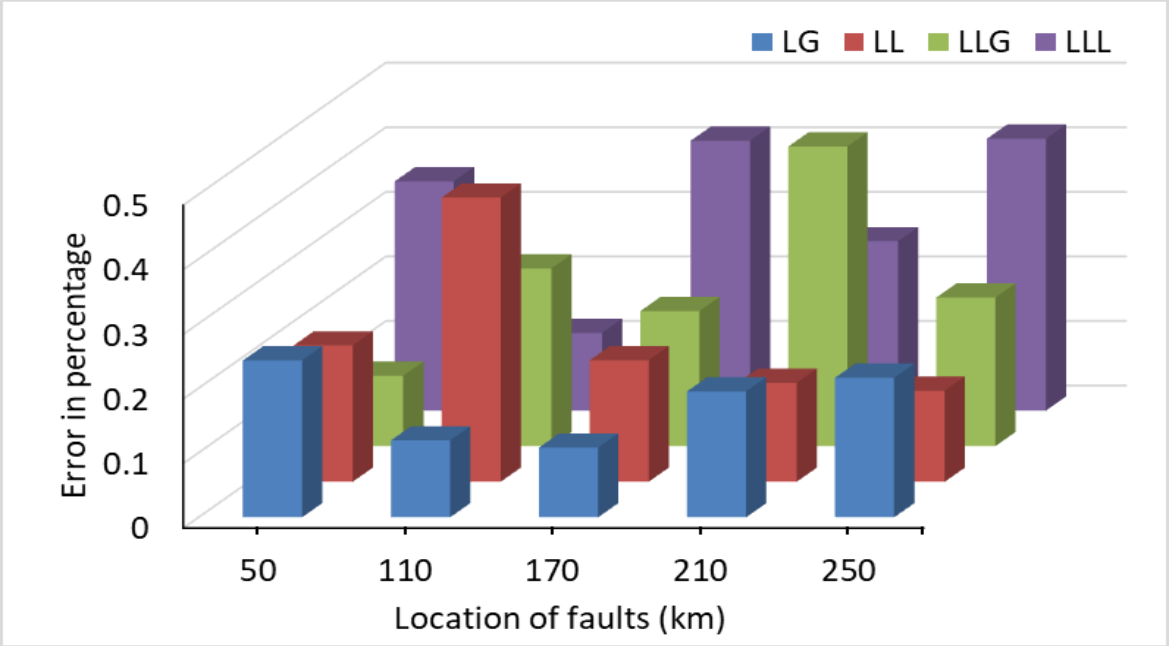

Figure 6.18 Distance estimation error percentage with respect to location of faults using CFNN

6.4.3 Test Case III: Series Compensated Parallel Transmission Network (Third test system)

The efficacy of the proposed CFNN model based fault distance estimating scheme has been also examined on simulated double circuit transmission system shown in Figure 6.19. It has been validated for various fault cases at different location in the simulated test system. Figure 6.20 represents the 3-phase post fault current samples retrieved during different fault cases in the first simulated test network at 30 km from the sending side. During the testing,

the features corresponding to all considered testing cases are fed to the trained distance estimator models. It predicts the location of the test fault case in the network as its output.

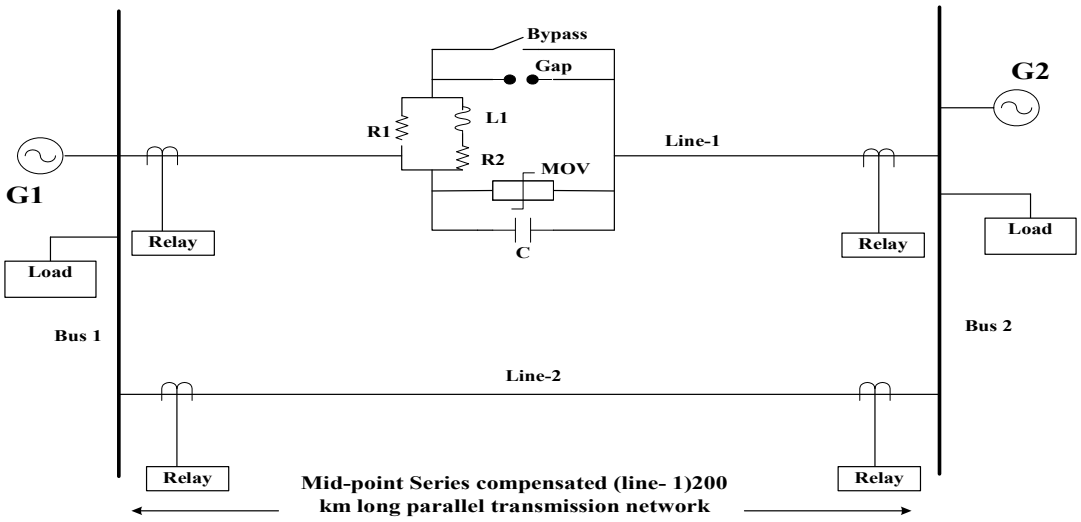

(a)

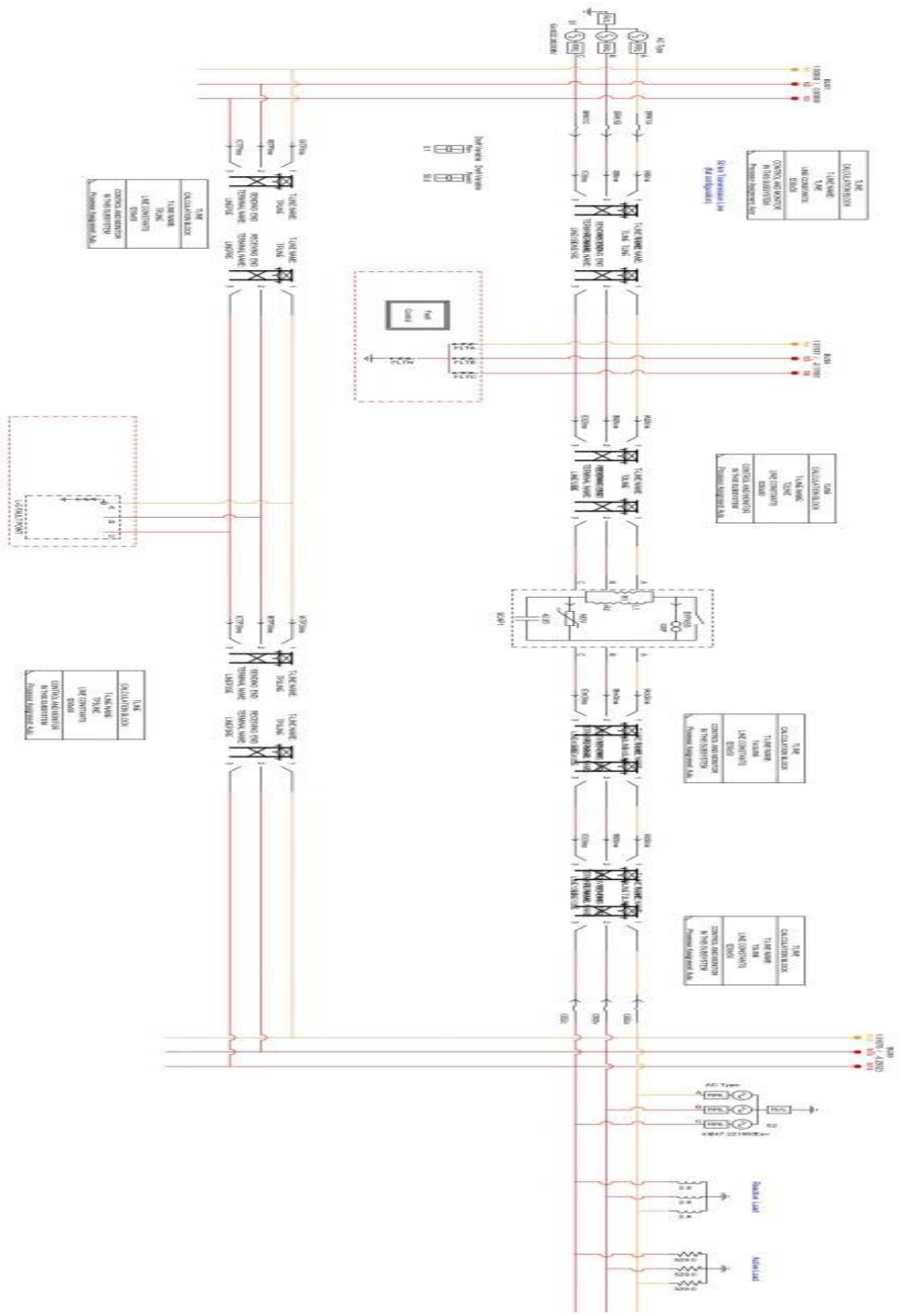

Figure 6.19 Simulated series compensated double circuit transmission (third test system) network; (a) single line diagram, (b) simulated test network in RTDS

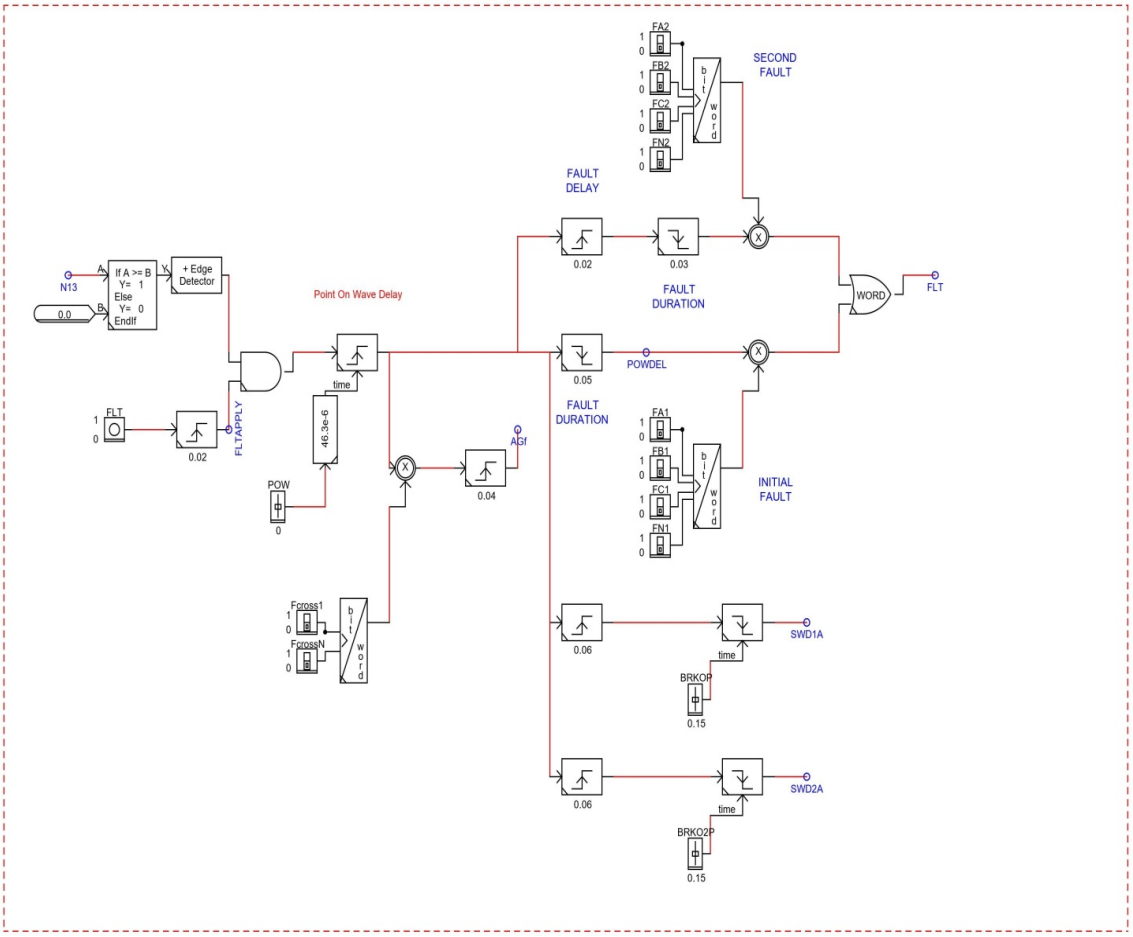

Figure 6.20 Logic diagram form simulating evolving and cross-country faults

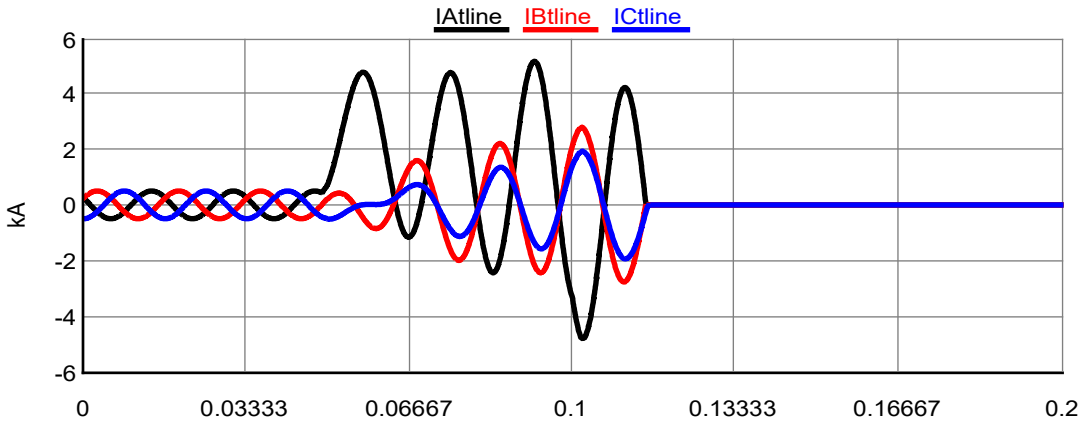

(a)

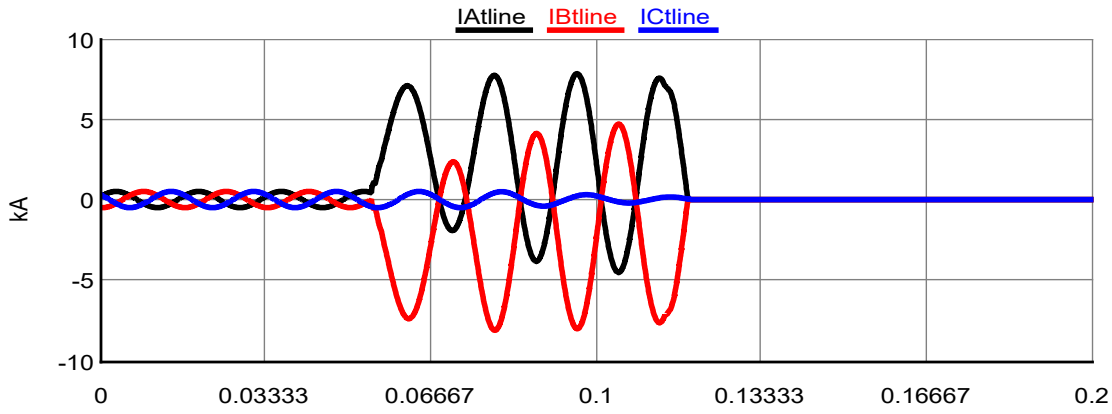

(b)

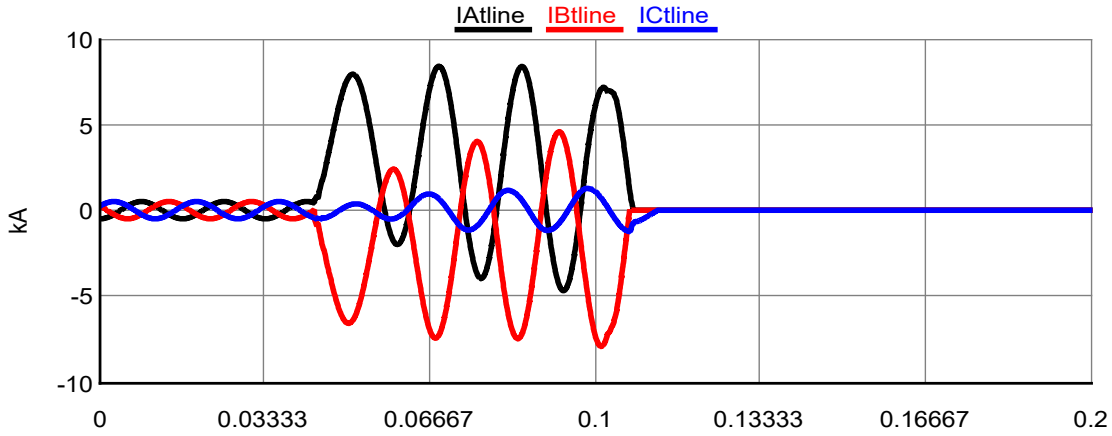

(c)

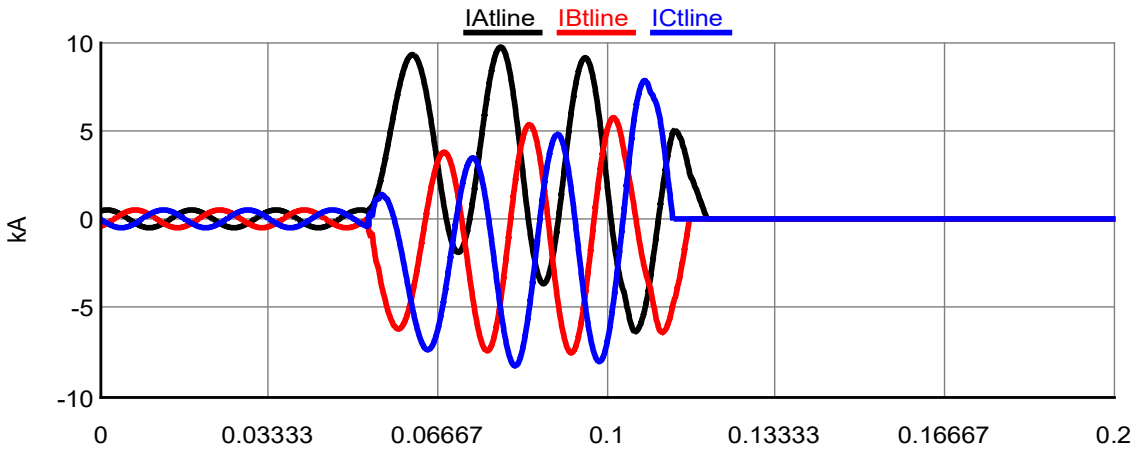

(d)

Figure 6.21 3-Phase current with respect to time (s) for different Fault events at 30 km (a) A-G event (b) A-B event (c) AB-G event (d) ABC event

Table 6.7 summarizes the fault distance estimation results and the corresponding estimation error percentage acquired by the proposed CFNN based distance estimating scheme. The obtained results clearly vindicated that the proposed CFNN based methodology is well competent in ascertaining the position of fault events in series compensated transmission system. Figure 6.21 represents the obtained error percentage during the tracing of different fault events in the simulated test network. The maximum distance assessment error is within 0.5 %.

Table 6.7 Fault events distance estimation using CFNN model on third test system

Type of fault	Actual location of fault	CFNN Model Output	Distance estimation Error (%)
Single line to ground fault	30	30.471	0.235
	50	49.082	0.459
	70	70.428	0.214
	130	130.339	0.169
	150	149.810	0.095
	170	169.320	0.340
Double line fault	30	30.530	0.265
	50	49.621	0.189
	70	70.207	0.103
	130	129. 460	0.270
	150	149. 357	0.321
	170	170.168	0.084
Double line to ground fault	30	30.331	0.165
	50	49.862	0.069
	70	70.426	0.213
	130	130.284	0.142
	150	150.294	0.147
	170	169.417	0.291

Three-phase fault	30	30.421	0.210
	50	49.205	0.397
	70	70.047	0.023
	130	130.653	0.326
	150	149.742	0.129
	170	170.236	0.118

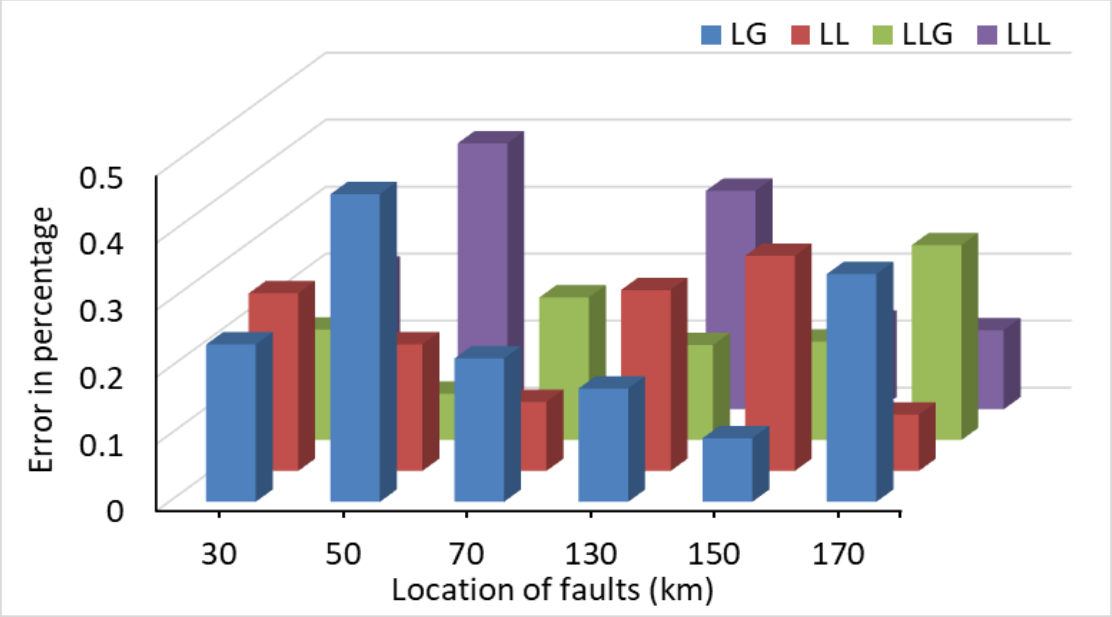

Figure 6.22 Distance estimation error percentage with respect to location of faults using CFNN model

6.5 Location of Evolving Fault Events

The efficacy of the proposed CFNN based model based fault distance estimating scheme is also examined for different evolving fault cases on second and third test systems. Authors in [121-123] have reported evolving fault localizing scheme in the power transmission circuit based on synchronized measurement and application of neural network. Figure 6.22-6.23 represents the 3-phase post fault current samples retrieved during evolving fault events

on simulated on second and third test system respectively. During the testing, the features corresponding to all considered evolving fault cases are fed to the trained distance estimator models. The CFNN model based distance estimator model predicts the location of the test instance in the network as its output.

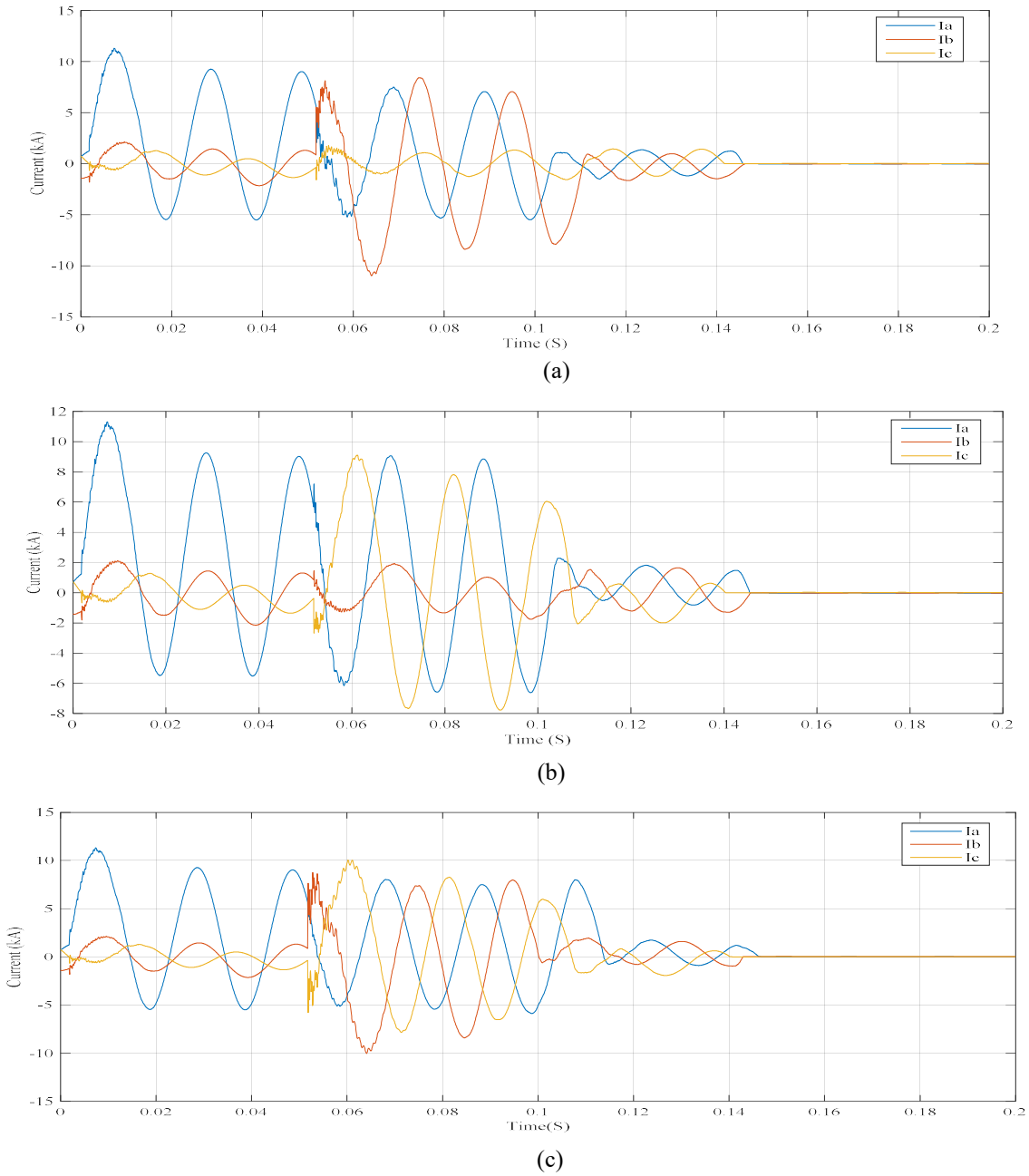

Figure 6.23 3-phase current samples during evolving fault in second test network (a) AG-bg at 50 km, (b) AG-cg at 50 km, (c) AG-abcg at 50 km

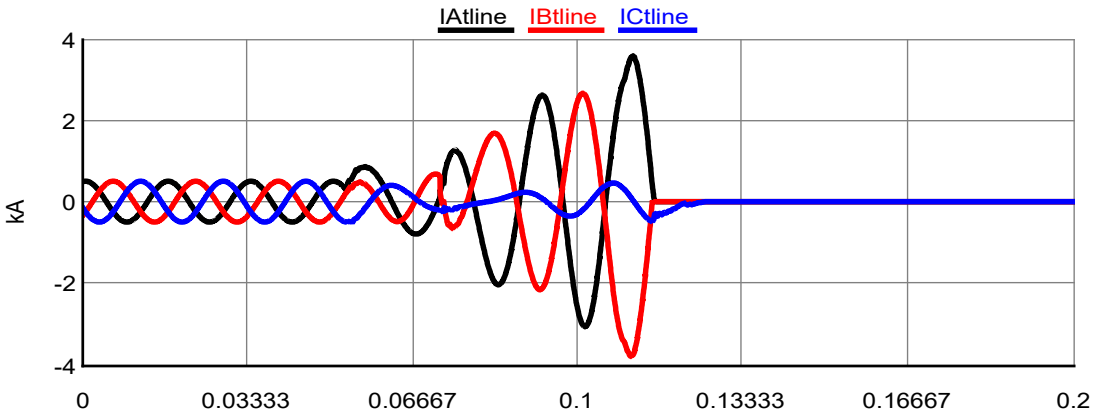

(a)

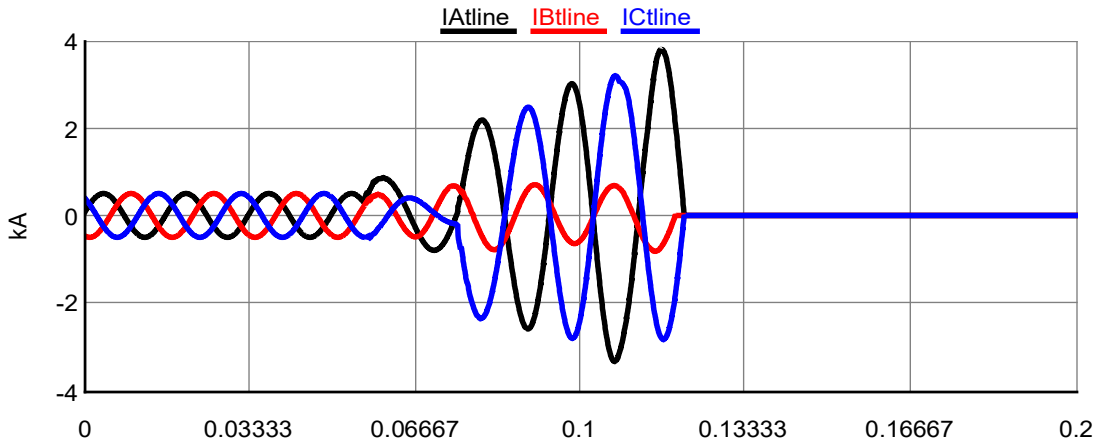

(b)

Figure 6.24 3-phase current samples during evolving fault in third test network
(a) AG-bg at 30 km, (b) AG-cg at 30 km

Table 6.8-6.9 summarizes the evolving fault distance estimation results and the associated estimation error percentage obtained by the proposed CFNN based distance estimating scheme during testing on second and third test system. The depicted result shows the relevance of the proposed CFNN model based methodology for localization the position of the fault events in the series compensated transmission system. Figure 6.24-6.25 represents the evolving fault distance estimation error percentage in the simulated test networks. The maximum distance assessment error is within 0.4 % for evolving fault events. Table 6.10

shows the comparative analysis of evolving fault distance estimation error obtained by the proposed scheme on second test system during testing and reported by some existing approaches. The error percentage by the proposed scheme is lowest as compared to that are reported in [121] 10 % error, [122] 3.06 % error and ± 1 % error in [123] respectively. Contrary to some already existing schemes for locating the EFE in the transmission network based on analytical circuit matrix analysis or communication channel based, the proposed scheme is simple and more accurate.

Table 6.8 Distance estimation of evolving faults CFNN based distance estimator model (second test system)

Evolving fault type	Actual location of fault	CFNN model Output	location estimation error (%)
Primary fault-AG Secondary fault-BG	50	50.146	0.048
	110	110.288	0.096
	170	171.087	0.362
	210	209.439	0.187
	250	250.646	0.215
Primary fault-AG Secondary fault-CG	50	49.572	0.142
	110	109.372	0.209
	170	170.756	0.252
	210	210.432	0.144
	250	249.150	0.283
Primary fault-AG Secondary fault-ABCG	50	50.237	0.079
	110	111.061	0.353
	170	170.713	0.237
	210	210.077	0.025
	250	249.578	0.140

Table 6.9 Distance estimation of evolving faults using CFNN based distance estimator model (third test system)

Type of Evolving fault	Actual location of fault	CFNN model Output	location estimation error (%)
Primary fault-AG Secondary fault-BG	30	30.168	0.084
	50	49.624	0.188
	70	170.436	0.218
	130	130.848	0.424
	150	149.347	0.326
	170	170.683	0.341
Primary fault-AG Secondary fault-CG	30	29.624	0.188
	50	49.262	0.369
	70	69.347	0.326
	130	130.324	0.166
	150	150.632	0.316
	170	169.350	0.325

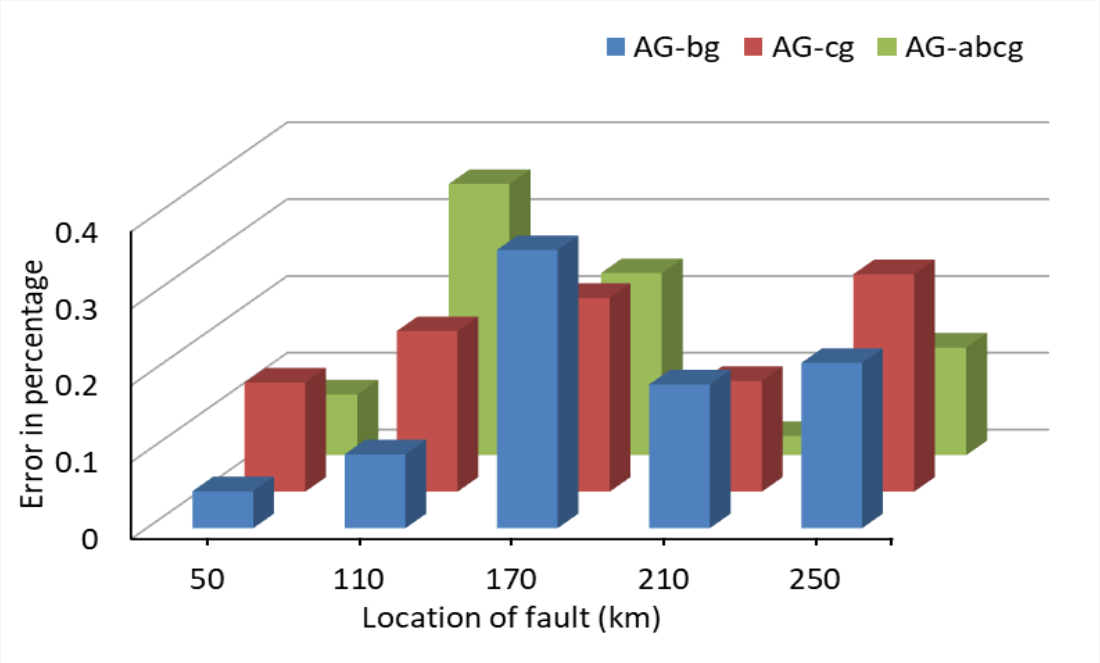

Figure 6.25 Distance estimation error percentage with respect to location of faults using CFNN model

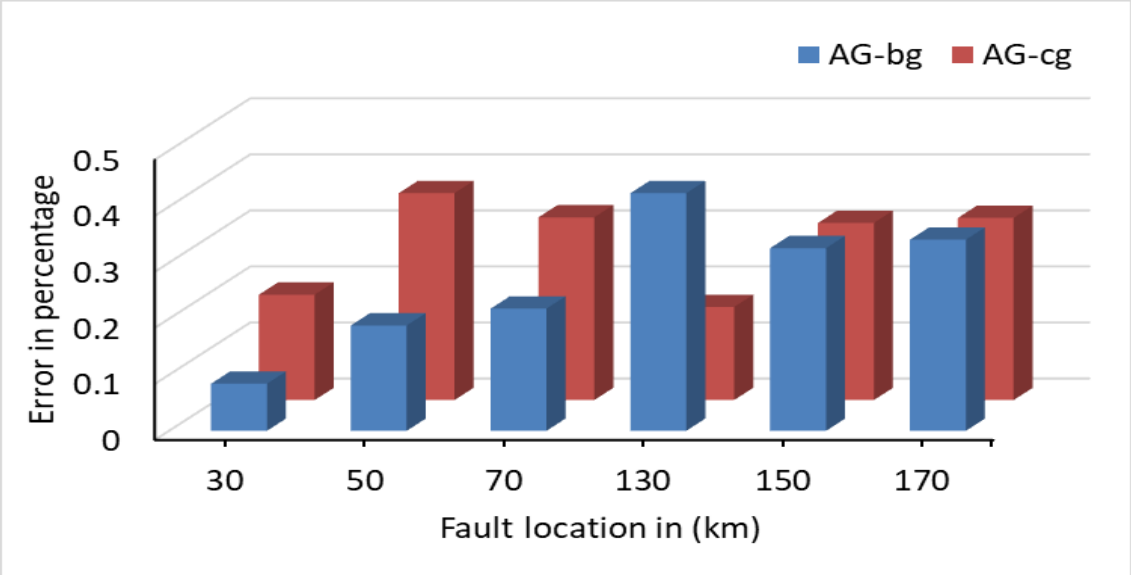

Figure 6.26 Distance estimation error percentage with respect to location of faults using CFNN model

Table 6.10 Comparision of distance estimation error for locating EFE in the network

Ref. No	Scheme applied	Measurement needed	Simulation Platform	Line compensation	Percentage error
[121]	Time domain analysis of primarily (LG) and subsequent LLG fault	Existing arc voltage during abnormality events	Real distributio n system	-	Location error within 10%
[122]	Phase domain network modeling based	Synchronized voltage and current signal at both ends	MATLAB	-	Location error within 3.06 %
[123]	DWT and ANN based	Both voltage and current samples	MATLAB	-	Location error within ± 1 %
Proposed scheme	DWT and cascade forward back propagation neural network based	3-phase current at one end	MATLAB	35% line compensation has been considered	Location error within 0.4 %

6.6 Conclusion

An integrated DWT and intelligent neural network based scheme has been presented in this chapter for estimating the fault distance in a series compensated transmission lines. The architecture and algorithms of the applied neural network based distance estimator models

are briefly covered. Later on, the feasibility and competency of the proposed fault distance estimating scheme has been validated on different simulated test systems. The results obtained by the proposed schemes for all considered test scenarios, has reaffirmed that the proposed schemes are well effectual in ascertaining the position of faults in series compensated power network.